



ENHANCED ANTIOXIDANT AND ANTIMICROBIAL ACTIVITIES OF SILYMARIN AFTER PARTICLE SIZE REDUCTION TO NANOMETER SCALE

Mujahid Sher^{1,2*}, Ishtiaq Hussain¹, Naila Gulfam³, Hamid Hussain Afridi⁴, Wiaam Mujahid Sher⁵, Muhammad Ateeq⁶, Farhat Ali Khan⁷, Muhammad Saqib Khalil^{6*}, Akhtar Aman⁸,
Mohammad Sulaiman⁹, Alija Baig¹⁰, Fawad Ali¹¹

¹Department of Pharmacy, Abbottabad University of Science and Technology, Abbottabad - Pakistan. Orcid.org/0000-0002-4594-9821. Email: mujahidss.aventis@gmail.com

¹Department of Pharmacy, Abbottabad University of Science and Technology, Abbottabad - Pakistan. Email: ishtiaq.hussain@fbse.paf-iast.edu.pk

²Premier Institute of Health Management Sciences, Peshawar, KP, Pakistan

³Jinnah College for women, University of Peshawar, KP – Pakistan. Email: nailazoo@yahoo.com

⁴Department of Pharmacy, Shaheed Benazir Bhutto University Sheringal, Dir Upper 18000, - Pakistan. Email: hamid@sbbu.edu.pk.

⁵Khyber medical college, Peshawar KP - Pakistan, Email: wiaamsher16675@gmail.com

⁶Sarhad Institute of Allied Health Sciences, Sarhad University Of Science And Information Technology. ateeqbiochem@gmail.com

⁷Department of Pharmacy, Shaheed Benazir Bhutto University Sheringal, Dir Upper 18000 - Pakistan. Email: farhat@sbbu.edu.pk

^{6*}Sarhad Institute of Allied Health Sciences, Sarhad University of Science And Information Technology - Pakistan, Email: saqib.biotech@suit.edu.pk

⁸Department of Pharmacy, Shaheed Benazir Bhutto University Sheringal, Dir Upper 18000 – Pakistan, Email: dramanrph@sbbu.edu.pk.

⁹Jiangsu Center for Pharmacodynamics Research and Evaluation, China Pharmaceutical University, Nanjing - China. Email: drsulaiman66@gmail.com

¹⁰Lady Reading Hospital Peshawar - Pakistan, Email: alijabaig@gmail.com.

¹¹Institute of Biotechnology and Microbiology Bacha Khan University Charsadda – Pakistan, Email: fawadansi@gmail.com

Corresponding author: Mujahid Sher
Email: mujahidss.aventis@gmail.com

Co-corresponding Author: Muhammad Saqib Khalil
Email: saqib.biotech@suit.edu.pk

ABSTRACT

Resistance development by microbes to the currently available drugs has driven us to find new ways to tackle this problem. Therefore, scientists had to embark on the task to find phytochemicals that could be used for the said purpose. Plant based antimicrobials are incredibly effective at combating bacterial, fungal, protozoal, and viral diseases without causing harm to humans. Silybum marianum (L.), generally known as Milk Thistle, seeds and fruits contain silymarin which has many therapeutic applications, such as antioxidant, hepatoprotective, and antimicrobial actions. Silymarin is hydrophobic and very less water insoluble with a very low oral bioavailability hampering its

therapeutic effectiveness. We attempted to enhance its solubility and oral bioavailability by reducing particle size to nanometer using two methods EPN and APSP. Characterization studies proved the reduction in its particle size and conversion to amorphous state and the bioavailability studies showed improvement in its absorption. Antimicrobial studies showed enhanced zones of inhibition and a clear reduction in MIC, MBC values compared to silymarin in the unprocessed form. The radical scavenging activity of the nanoform also increased.

1-Introduction

A rise in antibiotic resistance by some bacterial strains has grown into a significant risk to public health [1] (KhamenehB.,2019). Resistance development by microbes to the currently available drugs has driven us to find new ways to tackle this problem. Therefore, scientists had to seek help from nature to expand naturally derived agents from plants with antibacterial activities and embarked on the task to find phytochemicals that could be used for the said purpose. Moreover, during pregnancy, the urinary tract infections probability is enhanced in women, especially in the people of under developed world. But the majority of antibiotics used to treat UTI are contraindicated for pregnant woman. Therefore, it becomes difficult for a doctor to treat such infections. However, plant based antimicrobials are incredibly effective at combating bacterial, fungal, protozoal, and viral diseases without causing any negative side effects or violating the aforementioned contraindication [2] (AdamczakA.,2019). Evidence suggests that some medicinal plants are very effective at treating these illnesses [1,2] (KhamenehB.,2019) AND (AdamczakA.,2019).

Silybum marianum (L.), generally known as St. Mary's Thistle or Milk Thistle is a key member of the Compositae family of medicinal herbs. The capital city of Peshawar, Khyber Pakhtoonkhwah, Pakistan, and Kashmir are home to the milk thistle plant. In Peshawar, it grows from June to August. It also naturally grows in southern Europe, northern Africa, and the Middle East. The plant's seeds and fruits mainly contain silymarin, its major therapeutic component. Silymarin composition in milk thistle may be affected by a variety of variables, including plant origin, culture, and processing. However, silybin is the most potent and prominent (60–70%) component of silymarin, which is a very effective therapeutic molecule. The other compounds are silychristin (20%), silydianin (10%), and isosilybin (5%) [3](KřenV.,2022). Standard extracts with 70–80% silymarin are typically used to give silymarin [4] (PendryBA.,2017).

More than 2,000 years have passed since milk thistle (silymarin) was first used as medicine. It has many therapeutic applications, including its antimicrobial actions. Reports have proved the antimicrobial properties of silymarin against many harmful bacteria and fungi [5](HaghshenasB.,2023). Its antimicrobial activities have been investigated against selected bacterial, yeast and mold strains. The results indicated that different silymarin concentrations exhibited different antimicrobial activities against various microbes. The authors noted that antimicrobial activity of different samples increased as silymarin concentration increased [6](AbdelazimAS.2017). A group of researchers explored silymarin's antifungal actions and tried to find its mechanism of action. The results showed that silymarin disturbed membrane structure and increased permeability of the membrane permitting a free access to any molecules of the size of 3.3 nm. In this way, the reactive oxygen species accumulated which can exert toxic effects on various components of cells and can certainly react with lipids of cellular membrane encouraging lipid peroxidation. The authors also noted the actions like membrane depolarization and K^+ leakage and observed their association with increased permeability of the membrane. They noted that silymarin decreased fungal membrane fluidity. Finally they suggested that silymarin's antifungal action mainly involves targeting the plasma membrane of fungi [7](YunDG.,2017). A different team produced silymarin nanoparticles to demonstrate the antimicrobial potential of the compound in contrast to gentamicin and silymarin that had not been processed. When compared to unprocessed silymarin and gentamycin, silymarin nanoparticles exhibited a unique, considerable inhibitory impact against certain resistant bacterial strains. The investigations proved that silymarin has considerable antibacterial potential and converting silymarin to nanoform further improves its

performance [8](AlshehriFS,2022). In a different investigation, the effectiveness of silymarin against the pathogenicity of *S. mutans* and the formation of caries in a rat model and *in vitro* conditions was examined. The study's findings, which claim that silymarin is a bactericide, support the use of the compound either alone or in conjunction with other substances to prevent dental caries [9] (AskariF,2020). According to another study, silymarin has shown impressive anti-giardia and anti-amoebic effects against the trophozoites of both *G. lamblia* and *E. histolytica* [10] (AhmedA,2016). Some findings have also pointed to its synergistic effects against various bacteria when used in combination with other antimicrobial drugs [11] (AntikaLD,2021).

Silymarin also has significant antioxidant and cell regenerating capabilities and has been used since ancient times as a hepatoprotective agent. Silymarin, by scavenging free radicals, stops the lipid peroxidation process that leads to liver damage. According to studies, silymarin's antioxidant action is also linked to its use in treating liver problems, for example, hepatitis and cirrhosis [12] (AdetuyiBO,2021).

Excessive free radical presence leads to oxidative stress and may enhance the risk of developing chronic diseases. Silymarin can reduce this risk through a variety of antioxidative mechanisms. These are inhibiting reactive oxygen species producing enzymes, which prevent free radical formation, scavenging free radicals, intestinal ion chelation, promoting protective molecule synthesis, and activating antioxidant enzymes [13] (SuraiPF,2015). The antioxidant properties of silymarin may also improve hepatic lipid homeostasis [14](AkhtarDH,2019). The ability of various compounds to scavenge free radicals tends to vary. Therefore, assessing the free radical scavenging capacities is critical for the development of nutraceuticals and functional foods. Numerous *in vivo* and *in vitro* studies recommend that silymarin can help improve the oxidative stress. The DPPH and ABTS free radical scavenging capacities of silymarin were investigated by two separate groups of researchers. First group determined silymarin free radical scavenging capacity through DPPH and ABTS values [15] (IsmailiSA,2016). The other group assessed four free radical scavenging capacities: DPPH, ORAC (oxygen radical absorbing capacity), HOSC (hydroxyl radical scavenging capacity), and ABTS [16] (ChoeU,2019). Both groups discovered a similar trend in DPPH and ABTS free radical scavenging capacity, and both received higher free radical scavenging results. In another study, researchers tested silymarin DPPH free radical scavenging capacity in five different concentrations and discovered a concentration dependent % inhibition respectively [17] (MalekinejadH,2012). The findings from a study suggest that silymarin can protect tissues from cisplatin toxicity by decreasing the effects of oxidative stress and boosting antioxidant enzymes [18] (DoğanD,2022). In a trial, Nile tilapia fish were fed for 50 days a diet supplemented with raw and nanoencapsulated silymarin in predetermined doses according to their body weights and subsequently exposed to AgNPs for 24 h. Malondialdehyde content, glutathione peroxidase activity, and plasma glucose were all affected by the raw silymarin and silymarin nanoparticles treatment when compared with the control groups. Based on afore mentioned parameters indices, silymarin in both states reduced AgNPs toxicity, but the nanoform of silymarin showed best results [19](VeisiS,2021). A study has shown both the central and peripheral neuroprotective effects of silymarin against docetaxel induced neurotoxicity in rats. The authors considered that the antioxidant and anti-apoptotic potential of silymarin may be the main factor responsible for the protective effect of silymarin against docetaxel induced neurotoxicity [20] (YardımcıA,2021). Silymarin as a potent antioxidant can protect sodium arsenite induced harmful effects on mitochondrial membrane potential, non-progressive motility, and viability of ram sperm by enhancing the ability of sperm's antioxidant defense system [21](EskandariF,2016). According to findings from various studies, silymarin has powerful free radical scavenging strength against various types of free radicals. Due to its antioxidant activity, based on these findings, silymarin may be used as an innovative pharmaceutical in complementary medicine for the prevention of chronic diseases.

Silymarin is a hydrophobic and water insoluble compound with a very low oral bioavailability and needs frequent and large doses [22] (AbenavoliL,2018). The poor and unreliable bioavailability of this valuable compound may hamper its therapeutic effectiveness. In fact, one major obstacle to

using these compounds to their full potential for treatment is their limited oral bioavailability [23](Zhu,H.J.,2013). Attempts to enhance the oral bioavailability of silymarin have improved our understanding of the pharmacokinetics, dosing, and possible drug interactions of silymarin and other similar molecules.

Many technological revolutions have occurred in the past two centuries, including the industrial revolution, the revolution in medicine, the information technology revolution, and the nanotechnology revolution. Nanotechnology deals with the use of science and technology to control materials at the molecular and atomic level [24] (TaranM.,2021). To work with matter at this level has enabled us to outline, process, and fashion materials in ways never possible before [25] (Vijayalakshmi2015). Nanotechnology is an enabler that has the potential to contribute across a wide range of scientific and technological frontiers. It is also applied in agriculture and the environment.

Nanotechnology used in drugs or diagnostic molecules is called nanomedicine, where nanoparticles are employed to improve and restore health [26] (Pang,Z.,2019). Nanoparticles are small particles that usually range in size from 1 to 100 nanometers. Nanoparticles may have quite distinct physical and chemical properties from their counterparts in larger materials. Due to their smaller sizes, nanoparticles have been shown to be particularly helpful in achieving high bioavailability for very hydrophobic substances.

According to the biopharmaceutical classification system, a great percentage of the drugs have low water solubility [27] (AbuzarSM.,2018), making it a challenge for such drugs to have acceptable oral bioavailability. It is difficult to formulate these compounds using standard methods because these will have a number of performance related problems. The pharmaceutical industry is concerned about drugability due to unpredictable dissolution and limited bioavailability of such hydrophobic compounds due to the growing frequency at which novel chemical entities that are less water soluble are being identified. For medications to be effective in vivo, their solubility, and the resulting bioavailability are crucial factors, particularly, the bioavailability of medications taken orally depends on their breakdown and solubility prior to gastrointestinal tract absorption [28] (AlqahtaniMS.,2021). The rate of a drug's dissolution in GI fluids—is a rate limiting stage in its absorption. Dissolution rate is a function of a drug's solubility and particle size. Therefore, the medication dissolution rate determines how quickly most drugs are absorbed. Dissolution is a kinetic process, and the phenomenon by which molecules leave a solid drug's surface and move into the solution phase around it [29] (Parmar18). Drug particle size, surface area, and crystal habit all have the greatest impact on the pace at which low water soluble drugs dissolve.

Over the past few decades, formulating poorly water soluble chemicals with a nanoparticulate method has developed from an idea to a realization whose utility is only now starting to be recognized. Nanotechnology has established itself as a crucial component of pharmaceutical sciences and contributes to improve the therapeutic efficacy of drugs. In order to address issues with poor solubility and low absorption and increase the therapeutic potential of pharmacological moieties, nanotechnology has gained momentum. It is exciting to witness how quickly advances in nanotechnology are opening the way for the development of novel nanomedicines, which have the potential to completely reinvent current treatment approaches. The integration of phytotherapy and nanotechnology at clinical level will boost pharmacological response and favorable clinical results for the ailing population [30](SherM.,2023). In contrast to the conventional approach, nanotechnology has many advantages, as this method of delivery has rapid therapeutic activity, a low dose, less patient variance, good patient compliance, enhanced bio distribution, and possibly fewer side effects for the patient. Because nanomedicines are easily and effectively absorbed into the bloodstream, their biological activity and mobility are greatly boosted.

In nanotechnology we reduce the particle size of active medicinal ingredients to the submicron range, achieved by using either a bottom-up method or a top-down technique [31](VermaV.,2021). Top down method uses high pressure homogenization and mechanical attrition such as jet milling, media milling [32] (Recharla,N.,2017), a common and old method in pharmaceuticals. However, this method demands high energy, there is possibility of impurities, and the fact that the particle size

is not under our full control. On the other hand, the bottom up methods such as nanoprecipitation approach is more capable to manufacture drug nanoparticles [33](Sharma,C.,2021). Nano range drug can easily be recrystallized using the anti-solvent crystallisation approach. This method of crystallisation can take the place of cooling and evaporative crystallisation since it is an environmentally benign method of separation and purification. This process requires a low operating temperature that is beneficial for heat sensitive materials, in this way, some pharmaceutical products may avoid degradation by eliminating the thermal energy. The choice of two miscible solvents is the primary principle in this methodology. The medicine should be soluble in the solvent but not in the antisolvent. A high degree of super saturation is caused by the immediate injection of a drug solution into an antisolvent because the solution of drug diffuses into the antisolvent quickly, which causes the precipitation of nanoscale drug particles [34](JogR,Burgess.2017). According to the reviewed literature, reduction of drug particles to nanometer size increase the total effective surface area, which enhance wettability process, and increase the dissolution rate. The diffusion layer thickness that surrounds drug particles is also reduced as a result of reduced particle size, increasing the gradient of concentration. All of these processes can make a less water soluble drug more bioavailable which is the ultimate goal of using modern nanotechnology in medicine. The technique may be safely and easily used for different types of drugs. In fact these techniques have already been tested for almost all major drug classes.

In order to increase the bioavailability of silymarin by converting it into nanoparticles, the present nanotechnology study was conceived as well along similar lines. Increasing the presence of silymarin at the target location is our important goal. After increasing bioavailability, this strategy may improve the effects of the therapy, increase patient compliance, and lessen the likelihood of harmful systemic reactions. EPN and APSP, two separate methods, were employed for manufacturing nanoparticles. They underwent several experiments and were characterized to make sure the best nanoparticles were obtained. Both silymarin in its unprocessed form and as nanoparticles were employed in these experiments. According to the findings of studies on silymarin, nanoparticles have more potent pharmacological effects than the unprocessed product. The results presented here demonstrate increases in the solubility, dissolution, and bioavailability of the nanoform of silymarin, which is highly encouraging. To choose the optimum method, the two different strategies employed for producing silymarin nanoparticles were compared to one another. This is the first study of its kind on silymarin, and it aims to increase the drug's water solubility and bioavailability using two different approaches.

Experimental Details

2. Experimental Details

Silymarin was acquired from the PCSIR Peshawar for this study. Methanol, ethanol, and n-hexane were purchased from BDH. Rats were bought from the NIH in Islamabad. From a market in Peshawar, acquired healthy rabbits.

2.1. Fabrication of nanoparticles

We prepared nanoparticles by two methods, Antisolvent Precipitation with Syringe Pump (APSP) and The Evaporative Precipitation of Nanosuspension (EPN).

2.1.1. Evaporative precipitation of nanosuspension

In the EPN approach, methanol was used as solvent and n-hexane as antisolvent to prepare nanoparticles. In this method, the saturated solution of silymarin was prepared in methanol which was rapidly added to n-hexane. It resulted in the formation of nanoparticles. It was continuously stirred during the mixing of solvent and antisolvent phases. The resulting mixtures were quickly evaporated using a rotary evaporator operating under a vacuum pump to acquire the nanoparticles [35] (KhanFA.,2016). In order to obtain the nanoparticles of best grade having required particle size, zeta potential and PDI, the experimental conditions like solvent antisolvent ratio and stirring speed were optimized throughout the process of nanoparticles preparation [36] (Mohamed MS.,

2020). For this purpose different ratios and stirring speeds were used in separate experiments as shown in Table 1.

Table 1. Experimental conditions optimization in EPN method

Sample	Stirring speed(rpm)	Solvent antisolvent ratio
SM-EPN-1	1500	1:20
SM-EPN-2	2000	1:20
SM-EPN-3	25000	1:20
SM-EPN-4	3000	1:20
SM-EPN-5	3000	1:15
SM-EPN-6	3000	1:10
SM-EPN-7	3000	1:10
SM-EPN-8	3000	1:10

Key, SM-EPN= Silymarin nanoparticles prepared by the evaporative precipitation of Nano suspension method

2.1.1.1. Experimental conditions optimization

2.1.1.1.1. Stirring speed

As given in Table 1, the stirring speed, as the first parameter to be optimized was evaluated between 1500 and 3000 rpm. While optimizing the stirring speed, we kept back the solvent antisolvent ratios constant. It was discovered that by increasing the stirring speed, the size of particles decreased. An optimum stirring speed of 3000 rpm was recorded as the suitable stirring speed we needed for the preparation of nanoparticles so that to have desired features. We also optimized the solvent antisolvent ratios to further control the size of prepared nanoparticles, while maintaining a constant stirring speed at 3000 rpm.

2.1.1.1.2. Solvent antisolvent ratio

The solvent antisolvent ratio can also impact the nanoparticles sizes, therefore, the second parameter to optimize after the stirring speed in EPN approach was optimization of the solvent antisolvent ratio. The ratios for solvent and antisolvent were tested from 1:20 to 1:10 (Table 1) while maintaining the speed of stirring constant. As this ratio is increased, the sizes of nanoparticles decrease [36] (MohamedMS.,2020), the drug quickly precipitating into nanoparticles after its solution is mixed to the antisolvent. More antisolvent results in greater nucleation rate and smaller nuclei. Diffusion distance for growing species grows, becoming the limiting step for the growth nucleus as antisolvent concentration rises in the subsequent growth [37,38] [KakranM.,2012Mar] AND (KakranM.,2012Jun).

2.1.2. Antisolvent precipitation with syringe pump

According to APSP approach, unprocessed silymarin was rendered soluble in 50 mL of ethanol before being delivered into the antisolvent phase. Silymarin solution was filled in syringe and immediately introduced into a certain volume of n-Hexane (antisolvent) with a 2 mL/min flow rate and was continuously stirred throughout the process. The nanoparticles were obtained by quickly evaporating the resulting nanosuspension by help of a rotary evaporator operating under vacuum [35] (KhanFA.,2016). In order to acquire nanoparticles possessing the best features, important parameters during the nanoparticles preparation process, like stirring speed, and solvent antisolvent ratios were optimized [36] (MohamedMS.,2020). The optimized stirring speed and solvent to antisolvent ratio were selected that resulted in the preparation of nanoparticles of required size and shape.

2.1.2.1. Optimization of experimental conditions

2.1.2.1.1. Stirring speed

The synthesis of nanoparticles using the APSP technique involved optimization of the experimental conditions (Table 2). The stirring speed was evaluated from 1500 to 3000 rpm, during which solvent antisolvent ratios were held constant. We observed that by increasing the stirring speed, the particle sizes decreased. While maintaining a stirring speed constant at 3000 rpm, solvent antisolvent ratios were also optimized in order to further control the size of the synthesized nanoparticles.

2.1.2.1.2. Solvent antisolvent ratio

The solvent antisolvent ratio is very important because it can affect the size of nanoparticles. As the solvent antisolvent ratio is increased, the particle size gets decreased. The drug quickly precipitates into nanoparticles when the solution of the drug is added into the antisolvent. The solvent to antisolvent ratios were assessed from 1:20 to 1:10 (Table 2) when the speed of stirring was constantly maintained at 3000rpm. The sizes of the drug particles drastically reduced when the solvent-antisolvent ratio was increased [36] (MohamedMS.,2020).

Table 2. APSP method, experimental conditions optimization

Sample	Stirring speed (rpm)	Solvent antisolvent ratio
SM-APSP-1	1500	1:20
SM-APSP-2	2000	1:20
SM-APSP-3	25000	1:20
SM-APSP-4	3000	1:20
SM-APSP-5	3000	1:15
SM-APSP-6	3000	1:10
SM-APSP-7	3000	1:10
SM-APSP-8	3000	1:10

Key to the table; SM-APSP= Silymarin nanoparticles prepared by the antisolvent precipitation with syringe pump method

2.2. Assay of the prepared nanoparticles

After preparation, the drug content of the nanoparticles was assessed. A previously described method was used for this purpose [39] [A.Campodónico,2001]. By using methanol, a standard sample solution with an end concentration of 0.033mg/mL, was prepared. A stock solution for the sample assay test was prepared by dissolving 33 mg of sample in a 100mL volumetric flask. It was added with 70 mL of methanol and sonicated for 5 minutes. Methanol was also used to make up the final volume to the desired level after sonication. After it was thoroughly mixed, it was filtered through a syringe filter of 0.02 µL bore. Methanol was used to further dilute it to a 0.033 mg/mL concentration after filtration. A spectrophotometer was employed to measure it for silymarin content at 286 nm. Methanol was used as blank in the experiment. Experiment results were obtained in triplicate.

2.3. Characterization

Employing modern characterization practices such as Scanning Electron Microscopy, FTIR, XRD, Zeta Sizer, and DSC, the prepared nanoparticles were characterized. These characterization procedures can give reliable results for products of this kind.

2.3.1. Scanning electron microscopy (SEM)

JOEL JSM-5910, Tokyo, Japan was employed in our experiment to find electron micrographs of the samples. The SEM method uses electrons in its place of light to form an output image [40] (SharmaS.,2019). When incident light contacts the samples surface, electrons are reflected and drawn to a detector in which, an algorithm transforms them into pictures. Varying accelerating

voltages and magnifications were tried to achieve the requisite micrograph resolution. Before the analysis, the instrument was vacuum dried and using a double sided adhesive tape, a few sample droplets were applied to the instrument's metallic stub. During the analysis, the system's working voltage stayed at 30 mA for two minutes, while the accelerating voltage stood at 20 kV.

2.3.2. Analysis with Zeta Sizer

Malvern Instruments, UK, Nano series ZS 90, was used to characterize the nanoparticles for sizes, polydispersity index, and zeta potential. It is considered a suitable instrument that can measure particles in the size range of three nanometers to three micrometers. Zeta sizer analysis can measure fluctuations in the strength of scattered light caused by random particle movement. The systems temperature was held at 25 °C, and ultra pure water was supplied to the nanoparticles to obtain the proper scattering intensity for analysis. Prior to analysis, the samples were dispersed well in the aqueous medium with ultra sonication. This helps to maintain the polydispersity index below 0.5 that is required during analysis. The samples were introduced to a specifically developed cuvette with the help of micropipette to perform the analysis.

2.3.3. X-ray Diffraction (XRD)

To collect the XRD pattern of unprocessed drug and drug nanoparticles, the PANalytical X'Pert Pro, (PANalytical, Almelo, Netherlands) X-ray diffractometer, was employed. This analysis can authenticate the crystalline form of matter and a change if any in that form. XRD analysis is a quick, nondestructive analysis method that scarcely requires sample preparation. For the nanoparticles, the sample holders employed were made of silicon, and for the unprocessed drug, plastic sample holders were employed. The machine was set to 40 kV voltage and an operating current of 30 mA. Angles of 5° and 40°, respectively, were chosen as the initial and final angle points at 2 θ . Throughout the procedure, each step's size and duration were 0.02o and 0.5 seconds, respectively [41] [C.Racault,1994].

2.3.4. Differential Scanning Calorimetry (DSC)

DSC investigation for all the samples was carried out employing Mettler Tolado 822e (Greifensee, Switzerland). The effects of particle size reduction on the thermal kinetics of both the unprocessed drug and the prepared nanoparticles can be assessed by Differential Scanning Calorimetry tests. Relating the enthalpy (ΔH) of the nanoparticles and its corresponding original sample gives information about their crystallinity [42] [B.Siekmann,1994]. Amounts equal to 5mg of each sample were put separately in an aluminum made pan in the sample chamber for analysis. An empty pan (having no sample) was also used as reference. While being exposed to nitrogen gas flow at 40 mL/minute, the pans were heated at the rate of 10°C/minute between 60 and 200°C [42][B.Siekmann,1994].

2.3.5. Fourier-Transform Infrared Spectroscopy (FTIR)

In the current analysis, Shimadzu IR Prestige-21 FTIR, Kyoto, Japan was employed to serve our purpose. This technique can give information about any potential interactions between the drug and the excipients used to prepare the nanoparticles. The spectra were collected between 400 and 4000/cm.

Samples were prepared by mixing 200–300 mg of potassium bromide (KBr) with 2–3 mg of the material to be tested and compressed with a compression machine to prepare transparent discs. The discs were put in sample container for analysis. The component compatibility of nanoparticles was determined by matching the nanoparticle peaks and patterns to those of the unprocessed drugs.

2.3.6. Spectrophotometric analysis

PharmaSpec 1700, a spectrophotometer from Shimadzu Tokyo, Japan, was employed for calculating solubility, percent dissolution, and conducting content analysis. After the sample and

reference standards had been diluted, the analysis was performed at the appropriate " λ_{\max} " (286 nm for silymarin in this study) [43] (KhanBA, 2021).

2.4. Solubility study

For the unprocessed silymarin and its nanoparticles, solubility tests were performed. The solubility of the nanoform was compared to the solubility of the unprocessed compound.

To determine their solubility, 200mg of unprocessed silymarin and silymarin nanoparticles were separately shifted to 25-mL volumetric glass flasks and mixed with known quantities of distilled water. The volumetric flasks were sealed with aluminum foil to prevent losses by evaporation of the solvent and positioned in the orbital shaker for 24 h, which was fixed at an agitating speed of 100 rpm and kept at 25°C. After that, the samples were left undisturbed for 72 hours. To separate any drug part that had not yet dissolved (≤ 0.02 micron size), from the drug constituent that had dissolved, the supernatant layer was filtered with a syringe filter (0.02 μm , Whatman nanotop). To determine silymarin solubility, the sample was analyzed at 286 nm after filtration, employing a spectrophotometer. Triplicate copies of the analysis' findings were collected [44] (Sahibzada, 2017).

2.5. Dosage form formulation of silymarin

Silymarin nanoparticles were formulated into a suitable dosage form. For this purpose, hard gelatin capsules are considered a suitable dosage form due to their processing simplicity. It basically involves a few straightforward steps, such as adding the medicinal product to the capsule body before sealing the cap to the body.

This dosage form can significantly conceal silymarin's extremely bitter and unpleasant taste. In order to adjust the ingredient mass to fit a size "3" capsule, lactose was also used as a diluent. Each capsule of unprocessed silymarin and its nanoparticle form was manufactured by combining 50 mg of the active drug with 100 mg of lactose. Immediately following mixing, capsules were manually poured into their shells and sealed.

2.6. *In Vitro* release study

For this experiment, the paddle apparatus (Apparatus II) method was employed. The device used in this method has a coated paddle that can reduce stirring produced turbulence. The paddle is vertically attached to a motor that revolves at a controlled and changeable speed. The dissolution flask has a round bottom, which also reduces turbulence in the dissolution medium when the sample is put inside. The apparatus is placed in a water bath, which has a constant temperature of 37°C. A step wise detail of this experiment is given below.

2.6.1. Sample preparation for the study

Separate tests for the unprocessed silymarin and silymarin nanoparticle capsules were performed in accordance with USP [45] [U.S.P.XXII, Md(1990)]. A six vessels apparatus, DT-80, Erweka, Germany (Apparatus II, USP), was utilized for this experiment. To each vessel, 900 mL of distilled water, pH 6.5, was added. The operating temperature was adjusted to 37°C \pm 0.5°C, and the agitating speed was held at 100 rpm. One capsule was added to each dissolution vessel. At 10, 20, 30, 40, 50, 60, 70, 80, and 90 minutes, five milliliters of dissolution media were drawn from each vessel and filtered through a 0.02 μm syringe filter, which was continuously changed out for new dissolution media to keep sink environments constant. Using distilled water, the sample was diluted to 100 mL after filtration and mixed well. It was diluted until a final concentration of 22.22 $\mu\text{g/mL}$ was obtained.

2.6.2. Standard preparation for the study

A standard stock solution of silymarin containing 0.225 mg/mL in methanol was produced in a 100 mL volumetric flask for the dissolution experiment. Water at pH 6.5 was used as a blank to measure the spectrophotometric absorbance of samples and the standard at a maximum of 286 nm.

The below formula was used to calculate the drug release percentage.

Equation-I

2.7. Stability study

Using a stability chamber, storage stability testing was carried out on the nanoparticles to determine their stability. Various aspects of nanoparticles were cautiously observed and examined throughout the storage experiment of 24 weeks (180 days) at different pre planned time intervals to determine their stability. For measuring their stability during storage, 1) The nanoparticles were kept at temperatures ranging from 5 to 45 degrees Celsius. 2) Nanoparticle stability was also checked at different acidic and basic pH ranges. 3) They were also stored for different time periods, and their stability was checked at intervals of 1, 30, 60, 90, 120, 150, and 180 days.

The samples were held back for 180 days at each temperature (5°C, 10°C, 15°C, 20, 25, 30, 35, 40, and 45°C) and checked for any physical changes. By analyzing the samples on a regular basis, the essential parameters were periodically checked at 1, 30, 60, 90, 120, 150, and 180 days. During periodic analysis, samples were tested at predetermined intervals to observe any effects of temperature, pH, and time of storage on the nanoparticles stability. For this purpose, the samples protected from light were divided into different sets based on our pre planned temperature and pH slabs to be used for stability testing of nanoparticles. Each group was labeled as per the temperature and pH against which it was undergoing analysis. The labeled lots of the samples were tested over 24 weeks for optimum solubility and examined for particle size diameter, and polydispersity index. In the same manner, the prepared nanoparticles were also monitored for the fundamental quality parameters when stored at different pH conditions, ranging from 1 to 13 on the Sorenson scale, and the data was recorded and analyzed for up to 24 weeks. To verify the effects of pH, temperature, and storage time period on the drugs, such as possible particle aggregation during 180 days of storage, the preparations were checked for drug release. The outcomes were presented in per cent of the drug released at that particular time interval. This is important to note that while analyzing the temperature effects on nanoparticle stability, their pH was kept constant at 6.5, and the temperature was kept constant at 25 0C when the nanoparticles were studied at various pH conditions. When testing the effect of time duration on storage stability, the nanoparticles were stored at 25 0C and 6.5 pH from the first to the last day of the stability experiment.

2.8. Bioavailability study

Bioavailability studies were performed on both the silymarin nanoparticles and the unprocessed silymarin, which were compared with each other. The experiment was carried out using the method of [46] [Wu,J.,2007]. In this experiment, two groups, each comprising six rabbits, were randomly arranged. The animals were kept in strict compliance with the animal care agreement with the university. 50 mg/kg of crude silymarin, or SM-APSP 50mg/kg b.w., was administered to every rabbit through oral gavage. The first group was administered with unprocessed silymarin at 50mg/kg b.w., and the second group was treated with SM-APSP (silymarin nanoparticles produced by the APSP method) at 50 mg/kg b.w. Feeding two SM-APSP-50 capsules to each rabbit, we used 12 SM-APSP-50 capsules in this experiment, as the prepared SM-APSP capsules contained 50 mg of the API. The unprocessed silymarin sample dose was adjusted in the same manner and administered to the test animals. Before receiving the samples, the animals were kept fasting for 12 hours with unlimited access to water. They were kept within the animal facility and had one ear closely clipped and cleaned with a pad of 70% isopropyl alcohol. An outer ear vein was used to draw two milliliters of blood at specified time points of "0" hours (pre-administration), 1hours, 1.5hours, 2hours, 4hours, 6hours, 8hours, 12hours, and finally 24 hour. Following the procedure used before, [46] [Wu,J.,2007] the blood was instantly centrifuged at 3,000g for twenty minutes, and the serum was kept frozen until further examination with a UV-visible spectrophotometer. Following the same procedure, blood samples were collected every week from alternate ears. Every test was conducted in triplicate.

2.9. *In vitro* Biological activities

Different *in vitro* biological studies such as antioxidant and antimicrobial studies were performed for silymarin nanoparticles. The effects of prepared nanoparticles were also compared with the respective original compound to find the extent of improvement in the effects of nanoparticles.

2.9.1. Antioxidant Activity

The "DPPH• free radical scavenging action" previously stated by Yamaguchi et al. (1998) [47](YamaguchiT.,1998) was used to assess the antioxidative capabilities of the formulated nanoparticles. Following this procedure, a mixture for the reaction that contained 1mL of the DPPH• solution (0.1 mmol/L in a volume of 95% ethanol) in a brown conical flask was combined with varying concentrations of the test samples to produce a series of concentrations (10, 25, 50, 75, and 100 µM). The prepared mixtures were incubated in a dark cabinet at room temperature for 30 minutes. Using a UV-Visible spectrophotometer, each of these solutions was examined at 517 nm against a blank after incubation. The outcomes were represented as triplicates. The reduction in DPPH• absorbance, which was used to calculate radical scavenging activity, was computed according to below formula:

Effects of scavenging (%) = $[1 - A_{\text{sample}}(517\text{nm}) / A_{\text{control}}(517\text{nm})] \times 100$

2.9.2. Antimicrobial Activities

The antimicrobial potential of the prepared nanoparticles and their respective unprocessed drugs were separately investigated against selected bacteria and fungi.

2.9.2.1. Antibacterial Activities

The antibacterial potential of the samples was investigated against below selected bacteria.

Test Organisms: The clinical isolates for antimicrobial investigation were obtained from the Microbiology Department of AUST Abbottabad.

Bacterial isolates tested in this research comprised of both Gram positive and Gram negative bacteria (details given in respective tables). All bacteria included in this work were sub-cultured in Nutrient agar (NA) for 48 h at 37°C.

Antibacterial activity of the given samples was estimated through paper disc diffusion method. The cultures were set at 0.5 McFarland turbidity standard before their inoculation onto NA dishes having a diameter of 15 cm. Each sample was independently diluted with DMSO to desired concentrations. Sterile filter paper discs of 6mm diameters, impregnated with 50µl of samples dilutions prepared in DMSO were applied on every cultured dish previously inoculated with 0.5 McFarland bacterial cultures. Latter these cultures were incubated at 37°C for 18 h. Similarly, ciprofloxacin or DMSO impregnated paper discs were also used in this experiment as the positive and negative controls respectively. A digital Vernier caliper was used to measure and determine the millimeter size of the zone of inhibition surrounding each paper disc in order to estimate the antibacterial potential of the drugs following incubation [48] (Doughari,2006). Each test was performed in triplicate.

2.9.2.2. Antifungal Activities

Antifungal action of the prepared nanoparticles and their respective unprocessed compounds were also separately evaluated against selected organisms.

Test Organisms

Fungal isolates used in the antifungal study included both Molds and Yeasts (find details in respective tables).

We used potato dextrose agar to test the antifungal potential of the samples. To determine antifungal activity, cultures of selected fungi were adjusted to a concentration of 10^6 cfu/ml.

The cultures were inoculated at Sabouraud Dextrose Agar (SDA) dishes. Sterile filter paper discs measuring 13 mm diameter, impregnated with 50µl of sample dilutions already prepared in DMSO were applied on every cultured dish by now inoculated with 10^6 cfu/ml fungal cultures.

Candida albicans cultures were incubated for 18 h at 37°C, the cultures of remaining fungi were kept for 48h at 31 ± 1°C. Paper discs impregnated with amphotericin B and DMSO were used as the positive or negative controls respectively. For evaluating the antibacterial activity, for each paper disc, the zone of inhibition was measured [48] (Doughari, 2006). Three replication experiments for each organism in each sample were carried out.

2.9.2.3. Determination of MIC and MBC/MFC.

The samples MIC was assessed for every test organism in triplicate. A loopful of the organisms to be tested and previously diluted to 0.5 McFarland turbidity standard (in case of bacteria) or 10⁶ cfu/ml (in case of fungi), was added to test tubes after 0.5ml of various sample concentrations were mixed with 2ml of nutrient broth. Same method was followed to test the organisms with positive and negative controls (ciprofloxacin and DMSO respectively for bacterial isolates and amphotericin B in case of fungi). Tubes of bacterial isolates were incubated at 37°C for 24 h whereas those with fungal isolates were incubated at 31 ± 1°C for 48 h. At the end of period of incubation, the tubes were looked at for turbidity to note bacterial and fungal growth.

In order to estimate MBC, a loopful of broth from the tubes used to determine the MIC was taken from those that showed no growth and streaked on sterile NA and SDA for bacteria or fungi respectively. Bacteria inoculated petri dishes were incubated at 37°C for 24 hours however those inoculated with fungi were kept for 48 h at 31 ± 1°C. After the period of incubation, the sample concentration, which allowed no visible growth, was noted as MBC or MFC for bacteria or fungi respectively [48] (Doughari, 2006).

3. Results and Discussion

Silymarin has been extensively investigated for the treatment of various disorders. Unfortunately, this treasurable compound is poorly aqueous soluble, which is a challenge because poor aqueous solubility results in poor oral bioavailability. To help solve this problem, scientists spent lots of effort developing new formulation strategies to address these issues. The objective of the current research is to synthesize silymarin nanoparticles using two separate techniques, EPN and APSP, to enhance their solubility and oral bioavailability.

3.1. Fabrication of nanoparticles

3.1.1. Evaporative precipitation of nanosuspension (EPN)

The EPN approach produced particles of nano size with stirring rates of 3000 rpm and a solvent antisolvent ratio of 1:10 (Table 1). When these requirements were met, the EPN technique produced silymarin nanoparticles with an average size of 161.19 ± 1.91 nm (Table 4).

3.1.2. Antisolvent precipitation with syringe pump (APSP)

According to the APSP method and its optimization procedure, the best stirring speed was noted at 3000 rpm, and the best solvent antisolvent ratio was noted as 1:10 (Table 2). When these conditions were fulfilled, the APSP method provided amazing results and we achieved nanoparticles with an average size of 69.12 ± 0.38 nm (Table 4). The nanoparticles prepared by the APSP technique had smaller and even sizes when compared to those obtained by the EPN method, which was also proved by the characterization study.

Comparing the results of both methods, the APSP method produced particles with the smallest particle sizes and narrowest particle size distribution. In contrast, the characterization investigations showed that the EPN method produced nanoparticles of lower quality. The SEM analysis showed that the nanoparticles manufactured using the EPN method were irregular and not homogenous, in contrast to those prepared using the APSP method. If we consider the results of particle size and morphology, particles prepared via the APSP method may be the best nanoparticles that we can fabricate. The nanoparticles made using the APSP technique also surpassed those made using the EPN method in solubility and dissolution experiments. Therefore, we selected the nanoparticles

produced using the APSP method to be prepared into capsules formulation and were used to further carry out the activities that were planned.

3.2. Assay of the prepared nanoparticles

The assay results for the drug content of silymarin nanoparticles are noted in Table 3. The capsules formulated from silymarin nanoparticles (SM-APSP) produced assay results of $98.82 \pm 0.91\%$, and the unprocessed silymarin had $95.61 \pm 0.48\%$ results. The results achieved in both cases are within the allowed limits for a formulation (90–110% content).

Table 3. Drug content unprocessed silymarin and SM-APSP

S. No.	Product	Result (%)
1	Unprocessed silymarin	95.61 ± 0.48
2	SM-APSP	98.82 ± 0.91

3.3. Characterization

3.3.1. SEM analysis

In this analysis, the morphology, sizes and size distribution of silymarin nanoparticles were investigated and recorded their pictographs. The SEM pictographs of silymarin nanoparticles prepared by the APSP method are shown in Figure 1 as the white dots. The SEM pictographs reveal that the synthesized nanoparticles exhibited a predominantly spherical shape.

SEM analysis was also performed for the nanoparticles prepared using the EPN method (SM-EPN) and their morphology, reduction in the size was recorded. Unlike the nanoparticles prepared by the APSP method (Figures 1a and 1c), SEM analysis showed that SM-EPN did not have even sizes, they were present as bunches and had wider size distribution (Figures 1b and 1d).

As previously also reported, with the reduction in size the surface area of particles increase significantly which can lead to enhancement in their solubility, rate of dissolution and the resulting bioavailability [44,49] (Sahibzada, 2017) AND (DiCostanzoA, 2019).

Figure 1. SEM pictographs of SM-APSP (a, c) and SM-EPN (b, d)

3.3.2. Analysis by Zeta Sizer

We also evaluated the dynamic size and surface potential of silymarin nanoparticles synthesized using the APSP method and the results presented in Table 4. The Table shows zeta potential, polydispersity index and mean particle sizes of silymarin nanoparticles. The zeta potential of SM-APSP was noted as -33.4 ± 1.2 mV, their polydispersity index was noted as 0.231 ± 0.01 , and their average particle sizes were noted as 69.12 ± 0.38 nm. When EPN method was used, we achieved nanoparticles having zeta potential of -24.4 ± 0.81 mV, their polydispersity index was noted as 0.122 ± 0.1 , and their average particle sizes were noted as 161.19 ± 1.91 nm (Table 4).

The magnitude of zeta potential can tell us about the stability of nanoparticles. Strongly charged particles with high zeta potential values will encourage redispersion and avoid aggregation of the particles because of repulsive forces, but if the nanoparticles are not strongly charged and have low zeta potential they may tend to do otherwise [50][NémethZ, 2022]. Generally, we consider ≥ 30 mV and ≤ 60 mV values as good and excellent for stability [50][NémethZ, 2022]. Here, a zeta potential of -33.4 ± 1.2 mV indicates monodisperse nanoparticles without aggregates.

However, the only absolute sign of nanoparticle stability is not just zeta potential values. The sizes of nanoparticle be able to likewise affect the vital characteristics of pharmaceuticals like their release kinetics and drug distribution. SM-APSP particles are nanosized, which is significant because reducing the size of particle can enhance their surface area and the surface free energy. These are the factors essential for augmenting the dissolvability and rate of release of drugs, resulting in increased drug bioavailability and pharmacological actions [51] (MahapatraAP, 2020).

The nanoparticles prepared using the APSP technique had the estimated zeta potential values (Table 4) within the optimal range. The PDI value is recorded below 0.50, indicating even sized particles. In the same way, a zeta potential value of -33.4 ± 1.2 mV for SM-APSP point toward stable

nanoparticles. Such zeta potential values for nanoparticles mean a greater repulsive force that will help avoid agglomeration of the prepared nanoparticles promoting their stability. Therefore, the prepared nanoparticles will have a longer shelf life.

Table 4. Particle size, Zeta potential, and PDI of SM-APSP/SM-EPN

Method used	Average size of particles (nm)	Zeta potential (mV)	PDI
SM-APSP	69.12 ± 0.38	-33.4 ± 1.2	0.231 ± 0.01
SM-EPN	161.19 ± 1.91	-24.4 ± 0.81	0.122 ± 0.1

3.3.3. X-ray Diffraction (XRD)

X-Ray Diffractometry analysis was also conducted for silymarin both in the unprocessed form and after converting to nanometer size. XRD analysis revealed that silymarin nanoparticles have weaker diffraction peaks and indicated reduced sharpness (Figure 2a), which means a semi crystalline form. It proves that SM-APSP is present in amorphous state and has decreased crystallinity (Figure 2a). On the other hand, the XRD analysis results of unprocessed silymarin exhibited intense and pointed diffraction peaks at 2θ of 11.75°, 23.8°, 26.25°, 26.85° and 28.29°. Such characteristic peaks when present illustrate crystalline form of a compound (as shown in Figure 2b). Therefore, according to the XRD analysis (Figure 2b), unprocessed silymarin is present in crystalline form. It has already been discovered that one characteristic of the nanoparticles' decreased crystallinity is the diminished intensity in the diffraction peaks [52] (Holder,C.2019).

Silymarin melting point was determined at approximately 166 °C, which is consistent with earlier findings [53] (TavanoL,AlfanoP,2011). SM-APSP demonstrated their melting point at 162 °C. The silymarin's diminished crystallinity and transformation into an amorphous state were likewise confirmed by the XRD investigation.

Figure 2. XRD diffractogram of SM-APSP (a) and SM-unprocessed (b)

When compounds are converted to amorphous state, their solubility increase and their release rate improve, which in due course increase their bioavailability [54] (ŠtukeljJ,SvanbäckS,2019). Amorphous materials have higher free energy unlike crystalline materials, therefore, they are proficiently soluble [55] [Bremmell,K.2019]. In order to improve the pharmaceuticals' solubility and dissolution, which will boost their bioavailability, we may say that a conversion to nanoscale sizes and a change in crystallinity are the most effective approaches [56] (M.Kakran(2010)).

3.3.4. Differential Scanning Calorimetry (DSC)

In DSC testing, the thermal kinetics of the synthesized nanoform and the unprocessed drug were examined in relation to the implications of particle size reduction. DSC approach is useful for thermal analysis of a widespread range of materials. The results obtained from the analysis are presented in Figure 3. When the compound's amorphous form was examined, it was found that the width had increased and the elevation of the melting point peak had slightly dropped.

When analyzing the samples using DSC (Figure 3), a clear endothermic peak (representing the crystallinity of the material) was discovered at melting point temperature (166°C) for the unprocessed drug, whereas the nanoform of silymarin demonstrated a melting point slightly lower than that of the unprocessed drug. A lower acute melting point of silymarin nanoparticles (the amorphous form) is because of the nanoparticles low packing density; as a result, a little increase in the breadth and a decrease in the elevation of the melting point peak can be observed. It is obvious that silymarin crystallinity reduced after being transformed into nanoparticle state because the peak seen in the instance of SM-APSP was wider and less precisely centered than that of the unprocessed silymarin. The lowering of melting point may be attributed to the conversion of the drug to a semi crystalline state, reduction in the particle size, and increased surface area, the most important parameters that can considerably impact the melting point temperature [43] (KhanBA,RashidF,2021).

It is established that the melting point temperature denoted by “T_m,” is significantly influenced by the size and surface area of the particles. When the lattice of a crystal breaks down due to heat, an

endothermic process is shown by the steep peak that is produced in the melting point region of the crystal. Enthalpy of fusion (ΔH) value is another metric that indicates whether a material is crystalline or not. Materials that are crystalline have higher ΔH values, and less crystalline materials or amorphous materials have lower enthalpy values compared to their respective unprocessed compounds [57] (Albariqi,A.H.,2021). The enthalpy (ΔH) values of the unprocessed silymarin sample and the sample of prepared nanoparticle state were also compared to determine the crystalline nature of the samples [58] [YingchoncharoenP.,2016].

Figure 3. DSC Analysis Results of unprocessed silymarin and SM-APSP

3.3.5. Fourier-Transform Infrared Spectroscopy

FTIR analysis was conducted for silymarin samples both in the unprocessed state and in the nanoform. The FTIR spectrum helps to identify the samples and the comparative evaluation of their vibrational frequencies. The vibrational changes in the materials are determined by the intermolecular interactions. The investigation points towards a spectrum obtained with many peaks of changeable intensities due to vibrational fluctuations that represent different functional groups. The infrared spectra of silymarin (unprocessed) and SM-APSP are displayed in Figure 4 a, b. The figure shows that all functional groups vibrate at specific frequencies, which are visible in the FTIR spectrum as distinct peaks of varying intensities [59] (YousafAM.,2019).

Figure 4. FTIR spectra of SM-APSP (a) and SM-unprocessed (b)

The results of the FTIR analyses of all the samples show that the chemical makeup of the sample in nanoparticle form is quite comparable to that of the sample in its unprocessed form. The FTIR analysis confirmed that the prepared nanoparticles still have their structural integrity and no new complex had developed within the constituent parts of silymarin.

3.4. Solubility study

We performed the solubility study to conclude the maximum solubility and solubility enhancement of the prepared nanoparticles. Figure 5 below shows solubility data acquired both from unprocessed and nanoparticle forms of silymarin in distilled water. SM-APSP solubility was noted at $413.3 \pm 02.31 \mu\text{g/mL}$ (Figure 5) and the solubility of unprocessed silymarin was recorded as $221.4 \pm 3.2\mu\text{g/mL}$. The data clearly shows that water solubility of silymarin in the nanoparticles state greatly increased compared to that of the unprocessed drug.

The solubility of SM-APSP improved because of definite reasons such as the transformation of silymarin into an amorphous state that is proven by the DSC studies. It is established that the less crystalline compounds are more soluble than crystalline compounds [44,56] (Sahibzada.,2017) AND (M.Kakran(2010)). Conversion of silymarin into nano scale particles leading to an increase in the drug surface area, enhanced wetting capacity, and surface free energy also helped. All the aforementioned processes as a group massively enhanced the dissolvability and rate of release of silymarin [44,56](Sahibzada.,2017) AND (M.Kakran(2010)).

Figure 5. Aqueous Solubility of unprocessed silymarin and SM-APSP

Key; SM-APSP= Silymarin nanoparticles prepared by the APSP method

3.5. *In vitro* dissolution study

The dissolution experiment for capsule formulations of both the unprocessed drug and SM-APSP was performed in distilled water at pH 6.5. According to the data (Table 5) the dissolution of unprocessed silymarin was very weak; however, silymarin in the nanoform (SM-APSP) showed a far better dissolution rate.

The sample withdrawn after 10 minutes since the start of the experiment from the respective vessels contained 16.86 % silymarin from the nanoform of capsules, compared to the 5.11 % of silymarin released from the unprocessed drug capsules. This trend persistently followed, and after 30 minutes, 69.11 % dissolution of the SM-APSP and 17.24% of the unprocessed drug was recorded. At the end of experiment, 100.0% of the SM-APSP and just 39.79% of the unprocessed drug were dissolved

within the same duration (Table 5). The data showed an enhanced dissolution of SM-APSP compared to unprocessed silymarin.

Table 5. *In vitro* dissolution profile of unprocessed silymarin and SM-APSP at pH 6.5

<i>In vitro</i> dissolution profile of unprocessed silymarin and SM-APSP		
Time (min)	SM-APSP	Unprocessed silymarin
	% of drug dissolved	
0	0.00	0.00
10	16.86	5.110
20	38.48	12.16
30	69.11	17.24
40	80.22	28.21
50	95.89	35.71
60	100.00	37.92
70	100.00	38.74
80	100.00	39.61
90	100.00	39.79

Dissolution of nanoparticles is enhanced because nanoparticles can make available larger surface area for wetting compared to the unprocessed drugs. Because of this, the drug is released more quickly, need less time to reach greater drug concentrations at the site of absorption. According to the Noyes-Whitney and Ostwald-Freundlich equations, the huge surface area of nanoparticles accelerates both the kinetics of dissolution and saturation solubility. These factors improve the drug's absorption rate and ultimate bioavailability.

There are some other reasons also, having more surface free energy due to conversion of the drug to amorphous state, reduced aggregation among particles, and a better wettability because of expanded superficial area [60] (Croissant,J.2020). Due to improvement in the drug's gumminess to the cell membrane caused by nanoparticles' small sizes, the bioavailability of poorly water soluble drugs can also vastly increase [61] (Ali,I.,2020). It is critical to address the problem of poor aqueous solubility of silymarin because solubility and dissolution are the rate limiting processes for a given drug. The improved solubility and dissolution rate of silymarin in the current investigation predicts an improved and faster rate of absorption and superior bioavailability [62] (S.M.H.2016). After conversion to the nano form, the particles' surface area increased and the diffusion layer got thinner, which led to a far better dissolution [63] (Kayaert,P2012), because dissolution rate has a straight line relationship to the surface area [64] (DaSilva,F.2020). The relationship between various factors that affect a drug's capacity to dissolve was earlier shown in Prandtl and Noyes Whitney's equation. The adjustment of such parameters as surface area, particle size, and hydrodynamic boundary layer resulted in enhanced dissolution of silymarin. The rate of dissolution is also explained by the equation presented by Nernst-Brunner:

Equation-II

According to equation-II, a size decrease alone can increase the drug release rate while maintaining equivalent physical features [65] [ChiLip,2014] [66](KumarM.,2019).

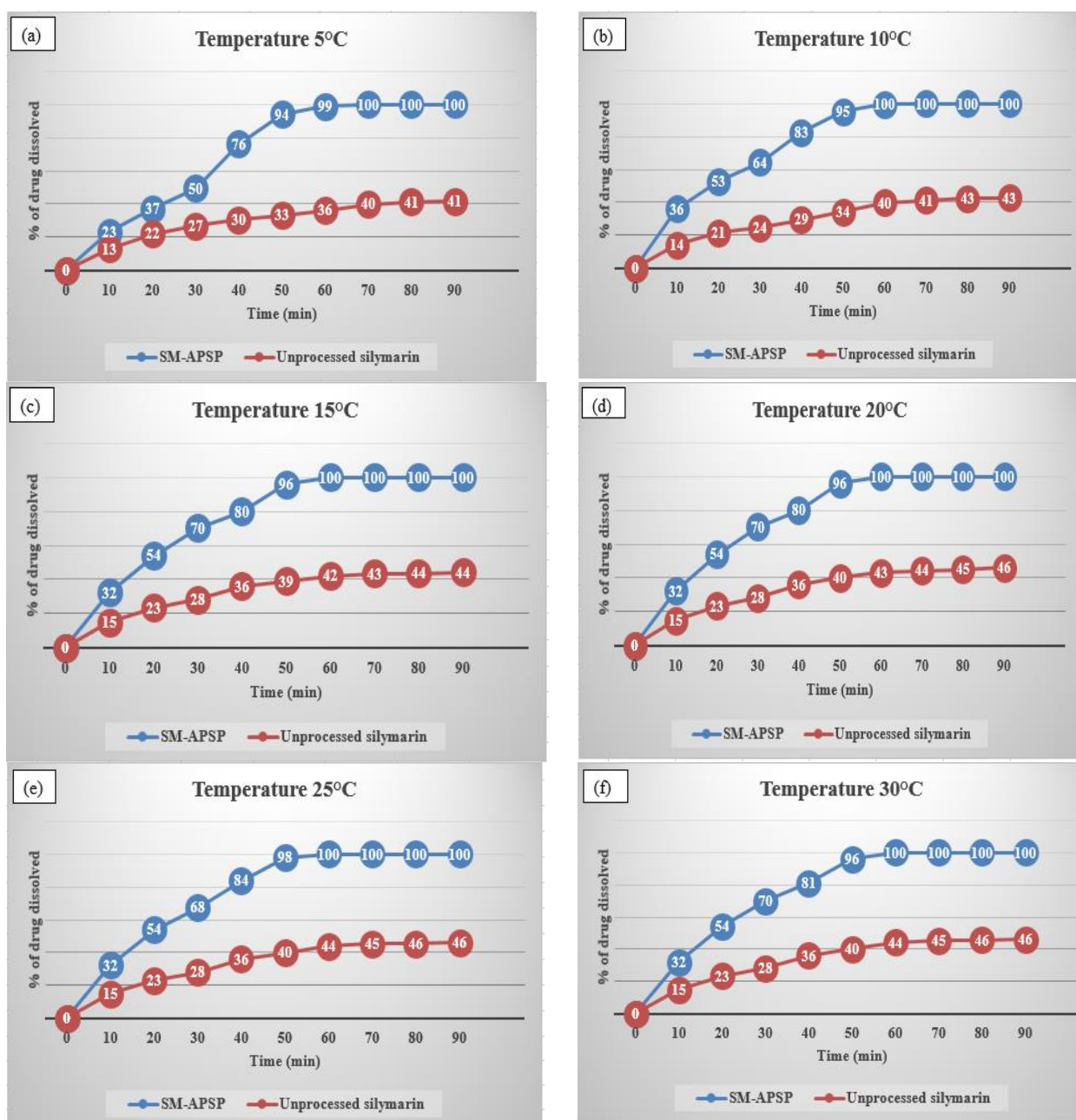
An enhanced pharmacological effect of a drug is possible if the drug reaches in larger amounts to the areas where its effects are needed [43] (KhanBA.,2021). More drug release leads to enhanced drug concentration at the site of action; therefore, SM-APSP may be recommended as a better alternative if there is a need to produce an enhanced pharmacological action.

3.6. Stability study

Stability of drugs has an important part to play in the procedures of drug development, transportation, and long-term storage. Therefore, silymarin nanoparticles were tracked to check on

their physical stability according to International Organization of Standardization (ISO) defined guidelines. Various important parameters related to the drugs stability like dissolution rates, drug content (percentage of drug), physical appearance of nanoparticles, and average particle sizes were all periodically monitored. While analyzing the effect of pH on nanoparticle stability, their temperature was kept constant at 25°C, and when testing temperature stability, the pH was kept constant at 6.5. Silymarin nanoparticles that proved most stable were set aside for further studies. The results of nanoparticles stability at different temperatures are presented in the Figure 6 and the outcomes from the samples stored at different pH levels are recorded in the Figure 7. The effects of time period on stability when the nanoparticles were stored at 25°C and pH 6.5 for different time durations are shown in the Figure 8.

The data demonstrates that nanoparticles remained stable at a wide temperature range of 5°C to 45°C (Figure 6a-i). The primary characteristics like particle size and dissolution rate did not change significantly. The dissolution of SM-APSP held at 5°C (Figure 6a) was 49.5%, and when stored at 45°C (Figure 6i), their dissolution was 48% in the first 30 minutes of the dissolution test. Unlike those, the nanoparticles that were stored at 25°C had dissolution rate of 68.2% in the first 30 minutes of the experiment (Figure 6e).



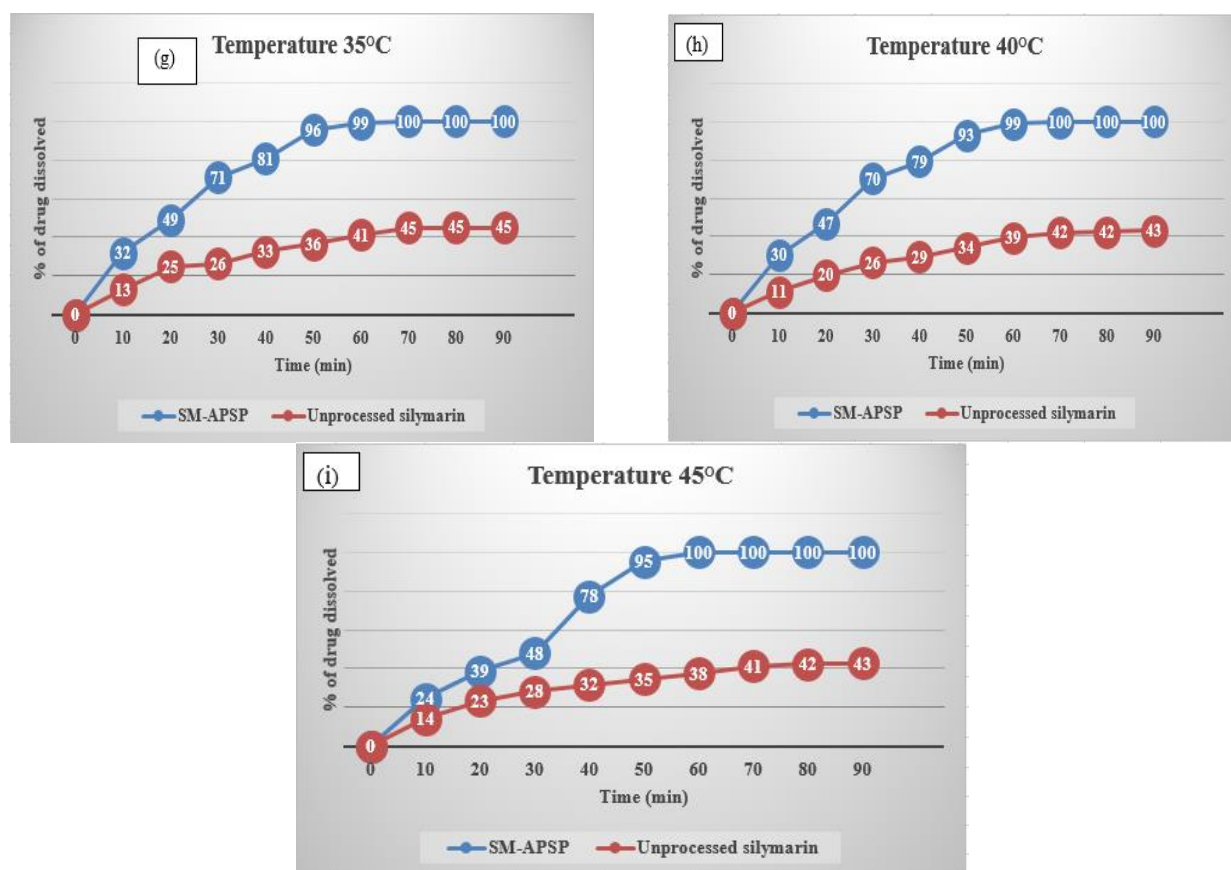


Figure 6. SM-APSP dissolution pattern of SM-APSP after storage at different temperatures

The data shows no appreciable modification in the dissolution rate of nano silymarin after storing for 24 weeks, except the minor changes in dissolution when stored at highest and lowest temperature limits. The lots stored at temperatures between 5°C and 30°C demonstrated excellent dissolution profiles, has also been reported previously [67](Pestovsky,Y.2018). The analysis of the nanoparticles stability at 5 °C to 30 °C revealed that the data derived from the dissolution of the nanoparticles during long term storage was not significantly different from each other when compared at different time points. The products had a desirable stability notwithstanding minor changes in certain cases, like a slight lumping effect, observed in samples stored at extreme temperatures. Such samples showed slightly lower rates of dissolution.

As the pH of a compound during storage and specially if stored for longer periods of time may also affect its stability [68] (Upadhyay,P.,2020), therefore, the nanoparticles stability under pH effects during storage for six months was carefully monitored and the data was collected (Figure 7). They were found stable at a wide pH range with no significant difference noted in nanoparticles dissolution rate and particle sizes, especially those stored at pH 5 to 7 (Figures 7c and 7d). The results are suggestive of homogeneous nanoparticles. However, it was noted that when the pH moved from 5 to 1 or from 7 onward, the nanoparticles became slightly clumped. As soon as the lumping effects happened at unfavourable storage conditions, the nanoparticles started to become micrometric and heterogeneous. Their dissolution behavior was also changed, showing slightly slower and incomplete dissolution. On the other hand, the samples held at pH 5 to 7 for up to 24 weeks remained stable. The slow dissolution of nanoparticles, particles size growth and their inability to maintain the initial diameters have also been previously reported for other compounds [69] (Piwowarczyk,.2022) [70] (PandeVV,.2016) [71] [Voorhees,PW.1985]. Therefore, the nanoparticles stability assessment is crucial because most materials when stored may experience some alterations that lead to sedimentation, cluster formation, growth of crystals, and even in some case, chemical reactions [72] (Kumar,D.2022).

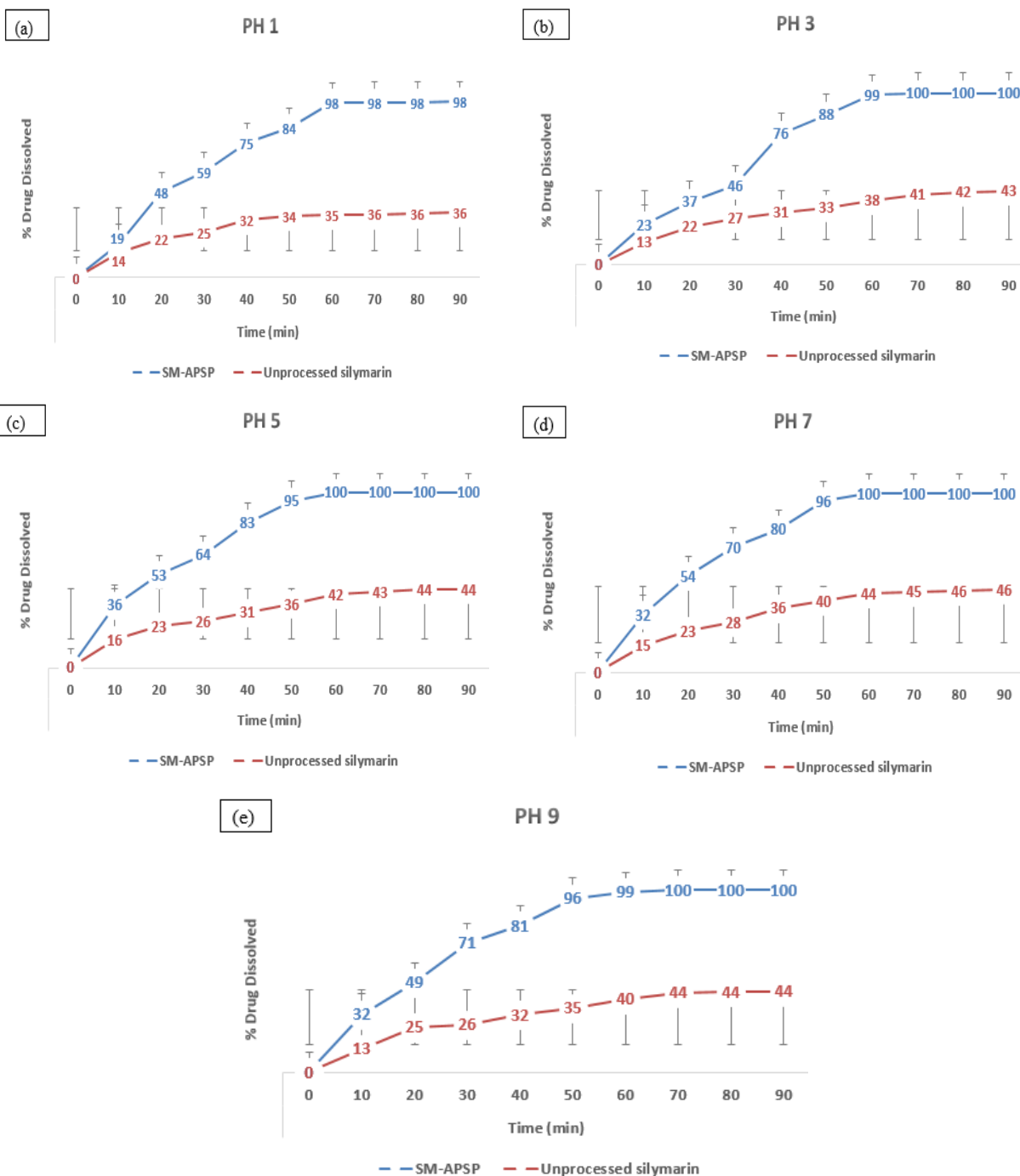


Figure 7. SM-APSP dissolution pattern after storage at pH 1 to 9

Finally, the nanoparticles were also stored at 25°C and pH 6.5 in suspension for up to 180 days and tested for quality parameters at predetermined intervals. The effects on nanoparticles stability and dissolution behavior were monitored and the data recorded (Figure 8a-g). No major changes were recorded in the particle sizes and dissolution rates during the analysis.

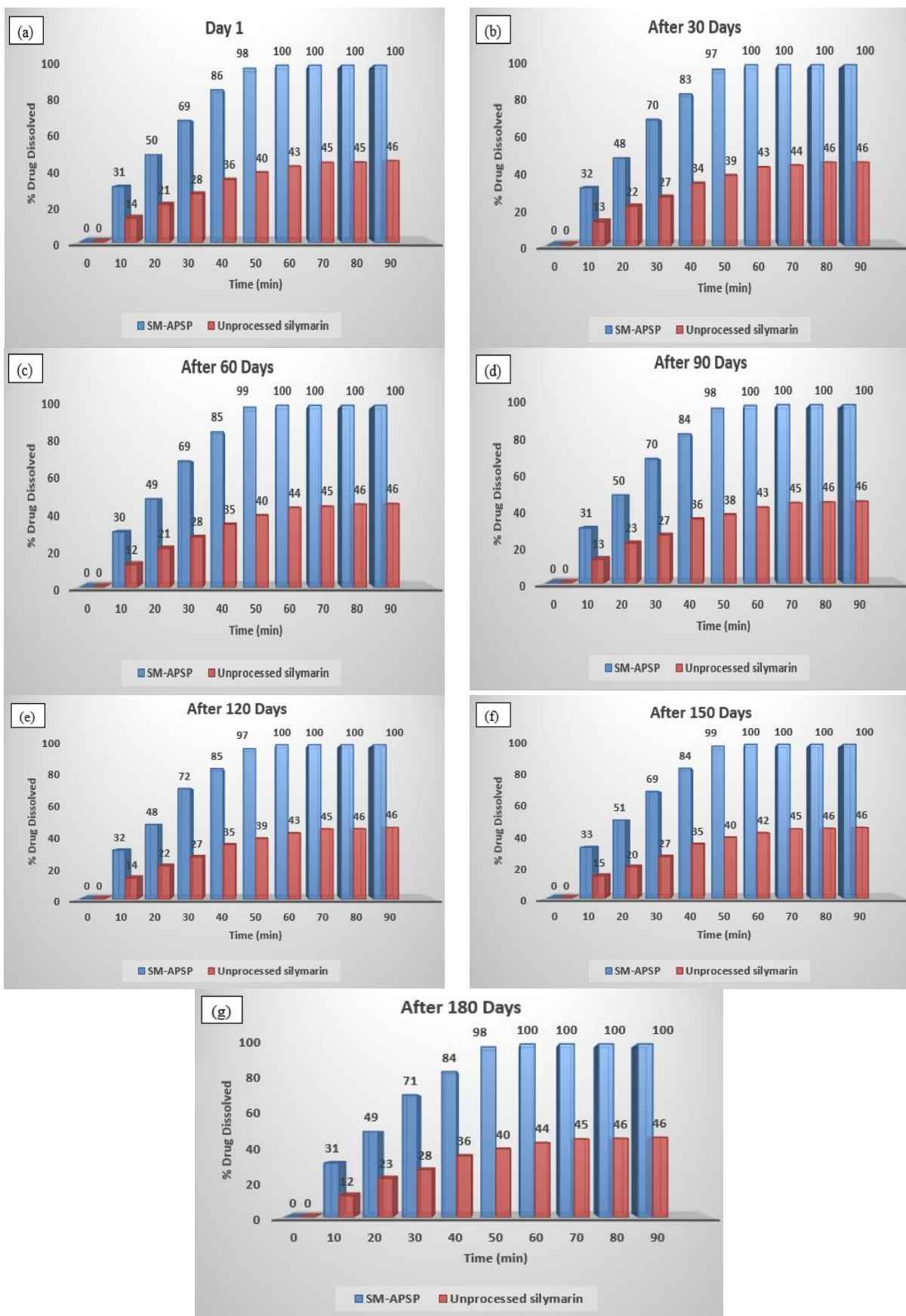


Figure 8. SM-APSP dissolution pattern from first day to 180th.day

Therefore, based on parameters like mean particle size and dissolution rate, it is resolved that the preferred temperature and pH ranges for storing silymarin nanoparticles are wide ranges of 5°C to 30°C and pH from 5 to 7 respectively. When stored at extreme pH and temperature conditions, they

revealed a modest increase in their sizes, however, not beyond 170 nm. The slight change in size with the passage of time at extreme temperature and pH conditions may be due to the agglomeration or merging of nanoparticles with each other [73] (Kaushik,M.,2019). The results obtained show that silymarin nanoparticles can remain stable for longer times if stored at recommended temperature and pH conditions.

3.7. Bioavailability study

The bioavailability of unprocessed silymarin and the improvement in bioavailability when it was converted to nanoparticles form was also assessed. The outcomes of comparing the bioavailability of silymarin nanoparticles to unprocessed silymarin demonstrate unambiguously that the nanoparticles have substantially better bioavailability. Figures 9, 10, 11, and 12 show the readings recorded for respective T_{max} , C_{max} ($\mu\text{g}/\text{mL}$), AUC ($\mu\text{g}\cdot\text{h}/\text{mL}$) and $t_{1/2}$ after administration of the samples of unprocessed silymarin and silymarin nanoparticles orally in the same doses to experimental animals. In the case of unprocessed silymarin, the maximum time in hours (T_{max}) to reach maximum plasma concentration (C_{max}) was 0.9 ± 0.36 hours (Figure 9), and it achieved a maximum concentration of 4.48 ± 0.20 ($\mu\text{g}/\text{mL}$). SM-APSP required $0.50 \pm 0.11\text{h}$ to acquire 20.86 ± 0.10 $\mu\text{g}/\text{mL}$ (C_{max}) as noted in Figure 10. Unprocessed silymarin and SM-APSP, achieved an AUC of 27.02 ± 1.92 ($\mu\text{g}\cdot\text{h}/\text{mL}$) and 279.73 ± 3.54 ($\mu\text{g}\cdot\text{h}/\text{mL}$) respectively (Figure 11). The figures illustrate that peak plasma concentration (C_{max}) achieved after SM-APSP administration was 4.65 greater, and area under the curve was 10.352 folds higher than those achieved with the unprocessed silymarin.

The results of the solubility study has also verified that the rate of dissolution of silymarin has enhanced considerably after conversion to nanometer size, which agree with the previous studies [74] [KesisoglouF,2007]. Particle size reduction results in increased surface free energy, a better wetting of the drug particles, and enhanced surface area, which collectively increase a compound's solubility and dissolution rate, both of which increase bioavailability. Silymarin conversion to nanometer range, enhanced surface area and its declining crystallinity are the major reasons for enhanced solubility [75](BhujbalSV,2021) that facilitated drug's release and absorption. The characterization results also supported this likelihood. Converting silymarin to nanoparticles form improved its *in vivo* absorption leading to a higher serum drug concentration, however, there were no significant differences between the $t_{1/2}$ of unprocessed silymarin and SM-APSP (Figure 12). The results achieved showing a higher bioavailability of SM-APSP than that of the unprocessed silymarin, are in agreement with the previous research [49,76] (DiCostanzoA,2019) AND (Tvrđý,V.,2021).

The above mentioned parameters (T_{max} , C_{max} ($\mu\text{g}/\text{mL}$), AUC ($\mu\text{g}\cdot\text{h}/\text{mL}$), and $t_{1/2}$) were calculated for all the test samples on the basis of blood data. The SM-APSP serum drug titers of the animals were found higher than those of the unprocessed silymarin. The superior bioavailability of SM-APSP than that of the unprocessed silymarin is because the nanoform is better than the unprocessed form in many ways [77] (AbdullahAS,SayedIE,2022). As silymarin is absorbed more quickly in the nanoparticle form than in the unprocessed form, the increased serum level of silymarin nanoparticles administered orally may be the result of particle size reduction [44] (Sahibzada,2017). The T_{max} for the nanoparticles was much shorter than the time required for unprocessed silymarin (0.5 ± 0.11 hours versus 0.90 ± 0.36) to reach C_{max} , which is in accordance with the previous studies [49,78] (DiCostanzoA,2019) AND (Javed,S.,2011). According to the data, SM-APSP achieved a higher peak serum level and a noticeably larger area under the concentration time curve in a shorter time (T_{max}) as compared to the unprocessed silymarin administered at the same doses. The C_{max} achieved by the nano form of silymarin SM-APSP (20.860 ± 0.100 $\mu\text{g}/\text{mL}$) is 4.65 folds higher compared to that of the unprocessed drug (4.48 ± 0.20 $\mu\text{g}/\text{mL}$).

The analyses demonstrate unequivocally that nanoparticles have many folds higher bioavailability than unprocessed silymarin; therefore, the strategy is successful. The findings suggest that nanoparticles might be a better choice for drug administration because they promote faster solubility and dissolution, which would lead to thorough and effective absorption—the findings that have also been proved earlier [79] (Pradhan,R.,2013).

The inadequate bioavailability of poorly water soluble compounds has been reported by many other authors as well and is linked to the poor absorption rate of the drug [80](Sahibzada.,2020). Drugs that are very marginally soluble, mostly have slow rates of dissolution, and typically have minimal bioavailability owing to poor *in vivo* absorption [81] (HedayaM.,2021). The association of low water solubility with poor oral bioavailability is logical because low aqueous solubility can hamper the bioavailability of unprocessed silymarin. These biopharmaceutical limitations necessitate that silymarin be transformed into a state which can sufficiently expand its bioavailability because the compound itself has significant clinical efficacy and needs attention. Because the drug cannot be made available at the target site in sufficient concentration to exert the required actions, the low bioavailability may result in therapy failure. Therefore, improving a drug's solubility and dissolution right from the beginning can improve its biopharmaceutical features, ensuring optimum therapeutic response [74] (KesisoglouF).

The increased drug surface area, which allowed for better saturation solubility and resulted in a thinner diffusion layer and quicker adherence to the cell membrane, led to a faster absorption of nanoparticles. In fact, the smaller the particle size, the greater the cell membrane adhesion, the greater the cell membrane adhesion, the better the saturation solubility which increases the drug saturation inside the cells. Similar reports about nanoparticles have also been put forward in other studies before [82] (Sahibzada.,2021). The smaller particle size also improve membrane permeability allowing more drug molecules to pass through [83] (Gupta,R.,2020). As advocated above, converting poor water soluble compounds to nanoparticle form appear to be a better substitute dosage form for silymarin and other poor aqueous soluble compounds to increase their oral bioavailability. The ease of preparation of such formulations and minimal requirement for basic ingredients are its standout qualities making them good candidates for industrial production.

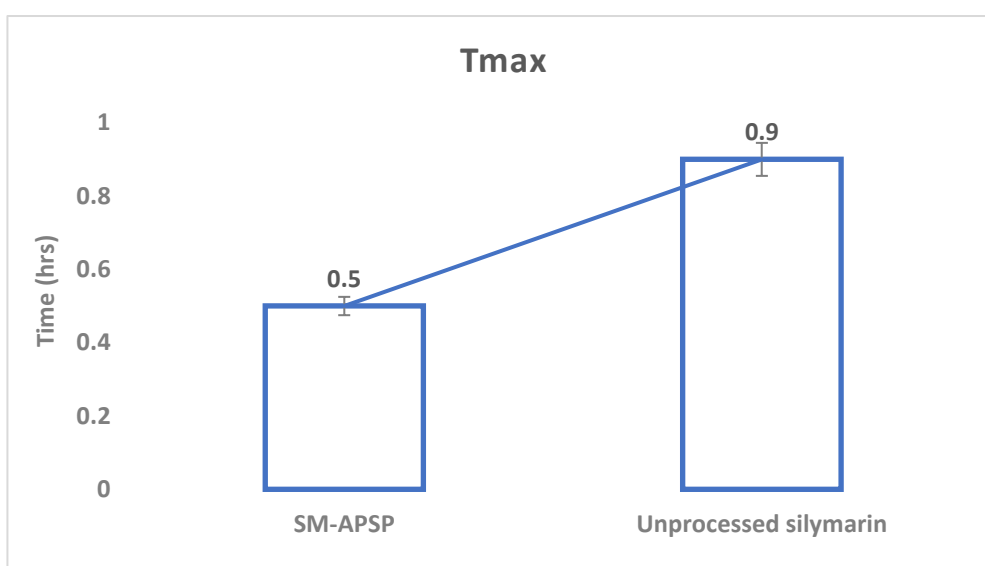


Figure 9. *In vivo* bioavailability study (T_{max}), unprocessed silymarin and SM-APSP

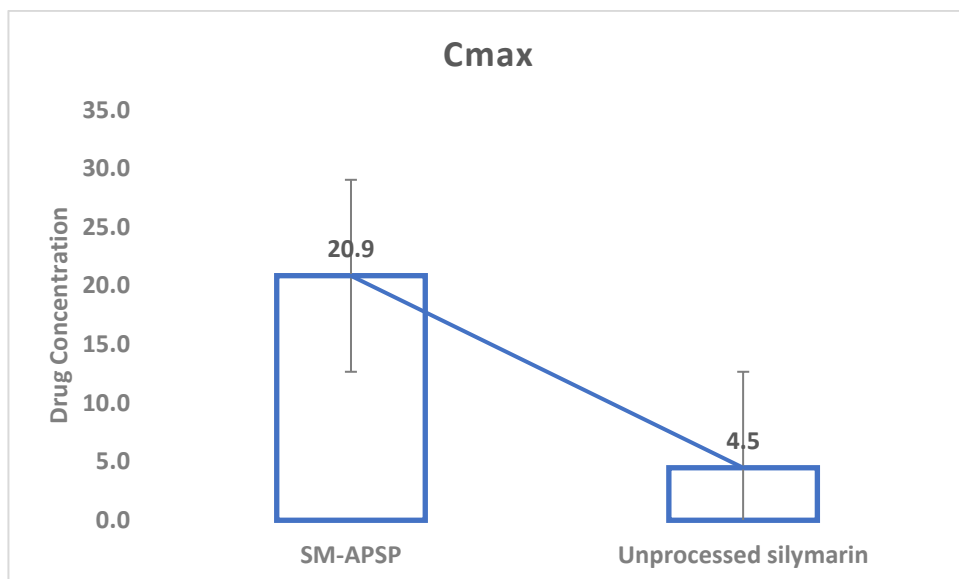


Figure 10. *In vivo* bioavailability study [C_{max} (µg/mL)], unprocessed silymarin and SM-APSP

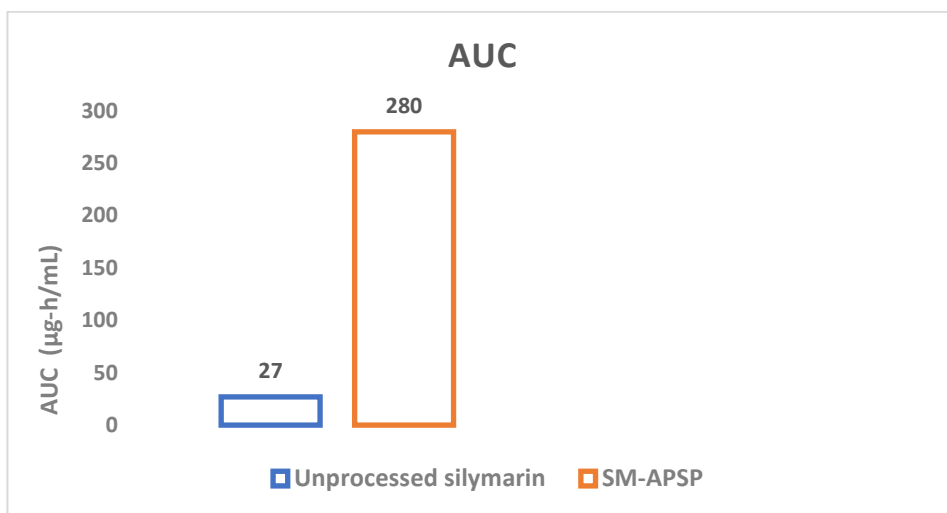


Figure 11. *In vivo* bioavailability study (AUC), unprocessed silymarin and SM-APSP

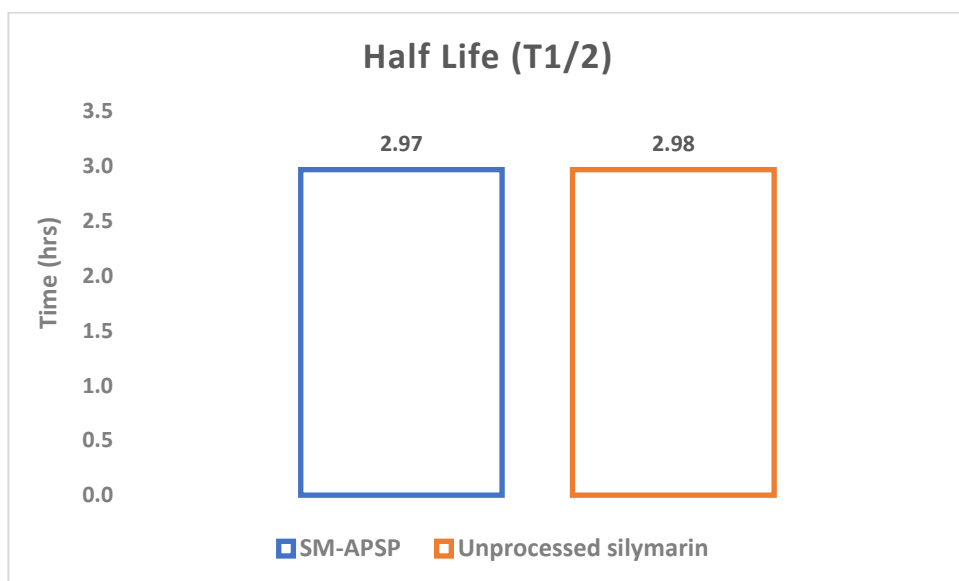


Figure 12. *In vivo* bioavailability study (half life), unprocessed silymarin and SM-APSP

2.8. *In vitro* Biological activities

3.8.1. Antioxidant activity

In medicinal use, antioxidant activities are generally due to the ability of compounds to demonstrate radical scavenging capacity [84] (MuflihahYM.,2021). The results presented in Table 6 indicate radical scavenging activity (% RSA) for silymarin and the nano drug (SM-APSP) at various concentrations.

A higher RSA% correlates to a higher antioxidant activity. Increasing the sample concentrations was discovered to be effective in improving the radical scavenging activity. Based on the data provided, the nanoform of silymarin has greater antioxidant capacity than unprocessed silymarin at all doses (10, 25, 50, 75, and 100 M). Silymarin nanoparticles prepared by the APSP method showed a 2.27 and 1.72 fold higher RSA at 10 μ M and 100 μ M, than that of the unprocessed silymarin. Therefore, by comparing the results to those of unprocessed drug, the prepared nanoparticles have higher antioxidant activity. All the samples had the ability to change the stable free radical 2, 2-diphenyl-1 picrylhydrazyl, into yellow diphenyl picryl hydrazine, however, the antioxidant activity of SM-APSP was far greater than that of the unprocessed silymarin. The activity of SM-APSP at 100 μ M was found to be the best out of all the samples tested and is closer to the values obtained from ascorbic acid.

The data shows that SM-APSP had a greater ability to scavenge DPPH• free radicals than the other tested sample and the inhibitory activities of unprocessed silymarin on free radicals were much lower than those of SM-APSP in all corresponding concentrations.

Table 6. Antioxidant activity of unprocessed silymarin and SM-APSP

Samples	10 μ M	25 μ M	50 μ M	75 μ M	100 μ M
SM-APSP-75	15.98 \pm 1.8	39.02 \pm 0.97	57.9 \pm 2.1	73.98 \pm 1.2	95.03 \pm 2.1
Unprocessed Silymarin	7.01 \pm 1.9	18.02 \pm 0.9	29.1 \pm 2.0	44.0 \pm 2.0	55.1 \pm 3.0

Key; Silymarin nanoparticles prepared by APSP method in 75 mg/kg b.w.

Antioxidant power, or the ability of antioxidants to scavenge free radicals and reduce compounds, is related to their antioxidant activity. In general, higher antioxidant activity is correlated with better reducing capacity. The majority of free radicals react with oxidizable substrates quickly due to their high reactivity.

In research, the highly stable organic radical based assay known as DPPH• has been extensively utilised to gauge how well different antioxidant compounds scavenge free radicals [85](SoraGT,2015), which is a common method for assessing the capability of an antioxidant compound to scavenge free radicals by employing DPPH• as a reagent. Numerous studies have pointed out a strong relationship between the bio functionalities and antioxidant activities of natural compounds. It is common practice to measure the bioactive components of medicines based on their antioxidant activity [86] (LiF,BoatengID.,2023). As evident from the experiment results, SM-APSP demonstrated the greatest DPPH• scavenging activity even tested in the same concentration. The tested samples having different particle sizes and crystal status could have affected their antioxidant activity. The greater antioxidant activity of the nanoform of the drug may bring a stronger *in vivo* response. This feature is the result of a more favourable pharmacokinetic profile; therefore, compared to unprocessed drugs, nanoparticles provide a better option as antioxidants.

Over the past so many years, silymarin has drawn a lot of interest as a natural treatment for several different ailments, including liver illness. A lot of the time, it's thought [87](KhanparaP.,2022) that silymarin antioxidant capabilities are what provide it its hepatoprotective effects. The body's antioxidant defense systems can be strengthened by silymarin through a variety of potential mechanisms [88] (AsgharpourM.,2021).

Silymarin has a lot of positive health impacts. It also proved itself a successful antioxidant in *in vitro* tests. The formulated silymarin nanoparticles may be useful for reducing or stopping the oxidative process in pharmaceutical items, delaying the production of harmful products of oxidation, preserving nutrient content, and extending drugs' shelf lives. Drugs with antioxidant

properties are used to prevent and treat complicated illnesses such cancer, diabetes, Alzheimer's disease, and atherosclerosis [89] (HegazyAM,2019) Therefore, it is crucial to identify the natural compounds, such as silymarin, that can be used as antioxidant. In this regard, the unprocessed silymarin and SM-APSP antioxidant potentials were compared.

The satisfactory reducing activity as exhibited by all samples is in line with previous studies [90,91] (ZimmerAR,2012) AND (ArampatzisDA,2019) however, the results shown by SM-APSP were the highest among silymarin samples ($23.1 \mu\text{g mL}^{-1}$) that can be attributed to its highly interactive nature due to the larger surface area resulting from the small particle size.

3.8.2. Antimicrobial activities

3.8.2.1. Antibacterial activity

Data in Table 7 shows the zones of inhibition achieved by unprocessed silymarin against various bacteria. The unprocessed silymarin recorded 9.24 ± 1.10 mm diameter of zone of inhibition against *Staphylococcus aureus* and 10.1 ± 0.91 mm zone of inhibition against *Streptococcus pneumoniae*. *Streptococcus pyogenes* showed a comparatively smaller zone of inhibition at 8.14 ± 0.88 mm and was found more resistant to the drug. Against *Staphylococcus epidermidis*, the zone of inhibition was recorded at 8.80 ± 0.5 mm. Silymarin achieved 8.04 ± 01.30 mm zone of inhibition against Vancomycin sensitive *Enterococcus* and 7.2 ± 0.91 mm against *Streptococcus viridians*, the later proving itself as the most resistant pathogen to silymarin in the unprocessed state out of all the six pathogens.

Against gram negative bacteria, unprocessed silymarin showed minimal activity. It achieved a zone of inhibition of 8.02 ± 1.2 mm against *E. coli* and was noted more sensitive than *Klebsiella pneumonia*, which had a zone of inhibition diameter at 7.04 ± 0.13 mm. *Enterobacter aerogenes*, recorded a zone of inhibition at 9.06 ± 0.64 mm, however, *Haemophilus influenza* was found more resistant and recorded a zone of inhibition at 7.11 ± 0.93 mm. The diameter of zone of inhibition against *Pseudomonas aeruginosa* was the smallest, and recorded at 5.7 ± 0.6 mm. *Proteus mirabilis* was found the second most resistant pathogen and recorded a zone of inhibition at 6.0 ± 0.3 mm.

Table 7. Antibacterial activity of unprocessed silymarin, zone of inhibition (mm)

Antibacterial activity of unprocessed silymarin					
Gram +ve bacteria	Zone of inhibition	Ciprofloxacin	Gram -ve bacteria	Zone of inhibition	Ciprofloxacin
Staphylococcus Aureus	09.24 ± 1.1	23.0 ± 0.03	Escherichia Coli	08.02 ± 1.20	27.01 ± 1.0
Streptococcus pneumoniae	10.1 ± 0.91	18.5 ± 0.80	Klebsiella pneumonia	07.04 ± 0.13	22.20 ± 1.0
Streptococcus pyogenes	08.14 ± 0.88	21.8 ± 0.20	Enterobacter aerogenes	09.06 ± 0.64	24.6 ± 1.03
Staph. Epidermidis	8.80 ± 0.50	21.8 ± 1.2	Haemophilus influenza	7.11 ± 0.93	21.8 ± 1.67
Vancomycin sensitive Enterococcus	8.04 ± 1.30	18.4 ± 0.02	Pseudomonas Aeruginosa	5.70 ± 0.6	24.2 ± 2.01
Streptococcus viridians	07.2 ± 0.91	17.8 ± 0.80	Proteus mirabilis	6.0 ± 0.30	19.30 ± 0.2

Minimum inhibitory concentration and minimum bactericidal concentration results of unprocessed silymarin are displayed in Tables 8 and 9, according to which, *Staph. Aureus* recorded an MIC of 186 ± 0.36 mg/mL and MBC of 393 ± 0.8 mg/mL. The MIC and MBC values for *Streptococcus pneumoniae* were recorded at 189 ± 0.88 mg/mL and 366 ± 2.2 mg/mL respectively. Similarly the respective MIC and MBC for *Streptococcus pyogenes* were noted as 194 ± 0.06 mg/mL and 347 ± 4.0 mg/mL. *Staph. Epidermidis* required the MIC as 164 ± 0.85 mg/mL and MBC as 332 ± 0.1 mg/mL. The MIC and MBC for Vancomycin sensitive *Enterococcus* were recorded at 181 ± 0.07

mg/mL and 368 ± 0.2 mg/mL respectively. *Streptococcus viridians* demonstrated MIC at 196 ± 1.61 mg/mL and MBC at 361 ± 0.9 mg/mL when treated with the unprocessed silymarin. In case of gram negative pathogens, the MIC and MBC values were noted higher than those required against gram positive pathogens. According to Tables 8 and 9, MIC for *Escherichia coli* was noted at 240 ± 3.05 mg/mL and its MBC was noted at 390 ± 3.5 mg/mL. When treated with unprocessed silymarin, *Klebsiella pneumoniae* demonstrated MIC, MBC values of 252 ± 1.31 mg/mL, 402 ± 1.3 mg/mL respectively. *Enterobacter aerogenes* recorded its MIC at 261 ± 0.90 mg/mL and MBC at 411 ± 0.9 mg/mL while the MIC and MBC values for *Haemophilus influenza* were noted at 253 ± 01.760 mg/mL and 400 ± 01.70 mg/mL respectively. The MIC and MBC values against *Pseudomonas aeruginosa* and *Proteus mirabilis* were noted as the highest and second highest among all the tested bacterial pathogens and were recorded as 268 ± 2.41 mg/mL MIC and 512 ± 2.4 mg/mL MBC for *Pseudomonas aeruginosa*, while 261 ± 2.27 mg/mL MIC and 411 ± 2.2 mg/mL MBC for *Proteus mirabilis* respectively.

Table 8. Minimum Inhibitory Concentration (MIC) of unprocessed silymarin (mg/mL)

Minimum Inhibitory Concentration of unprocessed silymarin (MIC) mg/mL					
Gram +ve bacteria	MIC	Ciprofloxacin	Gram -ve bacteria	MIC	Ciprofloxacin
Staph. Aureus	186 ± 0.36	1.24 ± 0.40	Escherichia Coli	240 ± 3.05	0.600 ± 0.11
Streptococcus pneumoniae	189 ± 0.88	2.0 ± 0.03	Klebsiella pneumonia	252 ± 1.31	0.85 ± 0.09
Streptococcus pyogenes	194 ± 0.06	0.39 ± 0.98	Enterobacter aerogenes	261 ± 0.90	1.50 ± 0.89
Staph. Epidermidis	164 ± 0.85	0.41 ± 0.07	Haemophilus influenza	253 ± 1.76	1.0 ± 0.26
Vancomycin sensitive Enterococcus	181 ± 0.07	0.97 ± 0.91	Pseudomonas Aeruginosa	268 ± 2.41	1.08 ± 0.20
Streptococcus viridians	196 ± 1.61	1.48 ± 1.04	Proteus mirabilis	261 ± 2.27	0.60 ± 0.98

Table 9. Minimum Bactericidal Concentration (MBC) of unprocessed silymarin (mg/mL)

Minimum Bactericidal Concentration of unprocessed silymarin (MBC) mg/mL					
Gram +ve bacteria	MBC	Ciprofloxacin	Gram +ve bacteria	MBC	Ciprofloxacin
S.aureus	393 ± 0.8	1.24 ± 0.40	Escherichia Coli	390 ± 3.5	0.600 ± 0.11
Streptococcus pneumoniae	366 ± 2.2	2.0 ± 0.03	Klebsiella pneumonia	402 ± 1.3	0.85 ± 0.09
S. pyogenes	347 ± 4.0	0.39 ± 0.98	Enterobacter aerogenes	411 ± 0.9	1.50 ± 0.89
Staph. Epidermidis	332 ± 0.1	0.41 ± 0.07	Haemophilus influenza	400 ± 1.7	1.0 ± 0.26
Vancomycin sensitive Enterococcus	368 ± 0.2	0.97 ± 0.91	Pseudomonas Aeruginosa	512 ± 2.4	0.81 ± 0.020
Streptococcus viridians	361 ± 0.9	1.48 ± 1.04	Proteus mirabilis	411 ± 2.2	0.69 ± 0.98

The nanoform of silymarin showed better activity against every tested bacterium compared to the unprocessed silymarin. Tables 7 and 10 show that the bacteria have significant dissimilarities among the diameters of the zones of inhibition in the unprocessed silymarin and SM-APSP groups. Depending on the zone of inhibition of SM-APSP, sensitivity results show that, except for *Enterobacter aerogenes*, generally gram positive bacteria showed more sensitivity than gram negative bacteria.

SM-APSP recorded 11.50 ± 0.14 mm zone of inhibition against *S. aureus*, which is wider compared to the unprocessed silymarin that exhibited 9.24 ± 1.10 mm zone of inhibition against this pathogen. SM-APSP showed better activity against *Streptococcus pneumoniae* and recorded a zone of inhibition at 12.16 ± 0.89 mm compared to the 10.1 ± 0.91 mm zone of inhibition demonstrated by unprocessed silymarin against the same pathogen. The diameter of the zone of inhibition against *Streptococcus pyogenes* for SM-APSP was noted at 10 ± 0.87 mm compared to the 8.14 ± 0.88 mm achieved by unprocessed silymarin. *Staphylococcus epidermidis* recorded a diameter of zone of inhibition at 10.2 ± 0.13 mm in the case of SM-APSP while the same pathogen demonstrated a zone of inhibition at 8.80 ± 0.5 mm when treated with unprocessed silymarin. SM-APSP recorded a zone of inhibition at 10.06 ± 1.10 mm in comparison to the 8.04 ± 1.30 mm zone of inhibition exhibited by the unprocessed drug against vancomycin sensitive *Enterococcus*. The zone of inhibition of SM-APSP was recorded at 10.34 ± 0.49 mm which is higher than the zone of inhibition recorded against *Streptococcus viridians* by the unprocessed silymarin (07.20 ± 0.910 mm).

Table 10 shows that SM-APSP also achieved higher zones of inhibition against gram -ve organisms compared to those achieved by unprocessed silymarin. The zone of inhibition of SM-APSP was noted at 9.2 ± 1.20 mm against *E. coli*, compared to the 8.02 ± 1.2 mm zone of inhibition exhibited by unprocessed silymarin. It demonstrated a zone of inhibition at 09.40 ± 3.10 mm against *K. pneumonia* compared to 7.04 ± 0.13 mm demonstrated by unprocessed silymarin. SM-APSP recorded 12.0 ± 1.10 mm zone of inhibition against *Enterobacter aerogenes*, which is higher than the 9.06 ± 0.64 mm noted for unprocessed silymarin against this pathogen. The zone of inhibition against *Haemophilus influenza* was noted at 8.74 ± 1.20 mm, which is again higher than the 7.110 ± 0.93 mm zone of inhibition recorded in case when *Haemophilus influenza* was treated with unprocessed silymarin. It is also greater than the 8.53 ± 1.2 mm zone of inhibition recorded against *Pseudomonas aeruginosa* when it was treated with silymarin in the nanoparticles form. *Proteus mirabilis* demonstrated zone of inhibition at 8.31 ± 0.10 mm when treated with SM-APSP, comparatively higher than when the same pathogen was treated with unprocessed silymarin. According to the results, *Streptococcus pneumoniae* is the most sensitive (12.16 ± 0.89 mm) bacterium to SM-APSP among all the pathogens. *Proteus mirabilis* and *Pseudomonas aeruginosa* stood out as the most resistant bacteria in the case of SM-APSP with respective diameters of zone of inhibition at 8.31 ± 0.10 mm and 8.50 ± 01.30 mm. *Klebsiella pneumoniae* (zone of inhibition diameter, 09.40 ± 03.10 mm) was found to be almost as sensitive as *E. coli* (9.20 ± 1.20 mm).

Table 10. Antibacterial activity of silymarin nanoparticles, zone of inhibition (mm)

Antibacterial activity of silymarin nanoparticles					
Gram +ve bacteria	Zone of inhibition (mm)	Ciprofloxacin	Gram -ve bacteria	Zone of inhibition (mm)	Ciprofloxacin
S.aureus	11.50 ± 0.14	23.0 ± 0.03	Escherichia Coli	9.20 ± 1.2	27.01 ± 1.0
Streptococcus pneumoniae	12.16 ± 0.89	14.5 ± 0.80	Klebsiella pneumonia	9.40 ± 3.1	22.20 ± 1.0
S. pyogenes	10.00 ± 0.87	21.8 ± 0.20	Enterobacter aerogenes	12.0 ± 1.10	24.6 ± 1.03
Staph. epidermidis	10.2 ± 0.13	21.8 ± 1.2	Haemophilus influenza	8.74 ± 1.20	21.8 ± 1.67
Vancomycin sensitive Enterococcus	10.06 ± 1.10	15.4 ± 0.02	Pseudomonas Aeruginosa	8.50 ± 1.30	24.2 ± 2.01
Streptococcus viridians	10.34 ± 0.49	16.2 ± 0.80	Proteus mirabilis	8.31 ± 0.10	19.30 ± 0.2

Tables 11 and 12 show the respective MIC and MBC results of SM-APSP. It recorded 122 ± 0.91 mg/mL and 105 ± 0.18 mg/mL MICs against *S.aureus* and *Streptococcus pneumoniae* respectively

with their respective MBCs as 316 ± 0.80 mg/mL and 256 ± 2.26 mg/mL. The MIC and MBC values against *S. pyogenes* were noted at 80 ± 0.07 mg/mL and 287 ± 3.08 mg/mL. The MIC recorded for *Staph. Epidermidis* was 112 ± 0.15 mg/mL, and its MBC value was 292 ± 0.150 mg/mL. and for Vancomycin sensitive *Enterococcus*, the MIC was noted at 79 ± 0.15 mg/mL (further on the lower side) with MBC value at 311 ± 0.15 mg/mL. Similarly, the MIC and MBC values for *Streptococcus viridans* were noted at 80 ± 0.71 mg/mL and 290 ± 0.71 mg/mL respectively.

Gram negative pathogens required higher MIC and MBC values compared to gram positive pathogens. The MIC and MBC values for *Escherichia coli* were recorded at 200 ± 0.71 mg/mL and 365 ± 0.71 mg/mL respectively. For *Klebsiella pneumonia* the respective MIC and MBC values were noted as 102 ± 1.42 mg/mL and 309 ± 1.42 mg/mL. According to Tables 11 and 12, *Enterobacter aerogenes* required 190 ± 0.09 mg/mL MIC and 310 ± 0.09 mg/mL MBC while the respective values of MIC and MBC against *Haemophilus influenzae* were recorded at 181 ± 0.83 mg/mL and 310 ± 0.83 mg/mL when treated with SM-APSP. MIC and MBC values against *Pseudomonas aeruginosa* were found highest among all the pathogens, noted at 204 ± 0.4 mg/mL and 371 ± 0.04 mg/mL respectively. *Proteus mirabilis* MIC was noted at 199 ± 0.88 mg/mL and it exhibited MBC value of 341 ± 0.88 mg/mL.

Table 11. Minimum Inhibitory Concentration of silymarin nanoparticles (mg/ mL)

Minimum Inhibitory Concentration of silymarin nanoparticles (MIC) mg/mL					
Gram +ve bacteria	MIC	Ciprofloxacin	Gram -ve bacteria	MIC	Ciprofloxacin
S.aureus	122 ± 0.91	1.24 ± 0.40	Escherichia Coli	200 ± 0.71	0.600 ± 0.11
Streptococcus pneumoniae	105 ± 0.18	2.0 ± 0.03	Klebsiella pneumonia	102 ± 1.42	0.85 ± 0.09
S. pyogenes	80 ± 0.07	0.39 ± 0.98	Enterobacter aerogenes	190 ± 0.09	1.50 ± 0.89
Staph. Epidermidis	112 ± 0.15	0.41 ± 0.07	Haemophilus influenza	181 ± 0.83	1.0 ± 0.26
Vancomycin sensitive Enterococcus	79 ± 0.15	0.97 ± 0.91	Pseudomonas Aeruginosa	204 ± 0.40	1.08 ± 0.20
Streptococcus viridans	80 ± 0.71	1.48 ± 1.04	Proteus mirabilis	199 ± 0.88	0.60 ± 0.98

Table 12. Minimum Bactericidal Concentration of silymarin nanoparticles (mg/mL)

Minimum Bactericidal Concentration of silymarin nanoparticles (MBC) mg/mL					
Gram +ve bacteria	MBC	Ciprofloxacin	Gram -ve bacteria	MBC	Ciprofloxacin
S.aureus	316 ± 0.80	1.24 ± 0.40	Escherichia Coli	365 ± 0.71	0.600 ± 0.11
Streptococcus pneumoniae	256 ± 2.26	2.0 ± 0.03	Klebsiella pneumonia	309 ± 1.42	0.85 ± 0.09
S. pyogenes	287 ± 3.08	0.39 ± 0.98	Enterobacter aerogenes	310 ± 0.09	1.50 ± 0.89
Staph. Epidermidis	292 ± 0.15	0.41 ± 0.07	Haemophilus influenza	310 ± 0.83	1.0 ± 0.26
Vancomycin sensitive Enterococcus	311 ± 0.15	0.97 ± 0.91	Pseudomonas Aeruginosa	371 ± 0.04	0.81 ± 0.020
Streptococcus viridans	290 ± 0.71	1.48 ± 1.04	Proteus mirabilis	341 ± 0.88	0.69 ± 0.98

3.8.2.2. Antifungal activities

For antifungal activity, Table 13 shows the diameters of the zone of inhibition recorded by unprocessed silymarin against selected moulds and yeasts. It achieved just 03.01 ± 0.1800 mm zone of inhibition against *Aspergillus niger* and 01.04 ± 0.100 mm against *Penicillium digitatum*. In case of *Fusarium oxysporum* and *Trichophyton rubrum*, it recorded zones of inhibition of 4.70 ± 0.89 mm diameter and 05.06 ± 0.10 mm diameter respectively. Although, this is not up to the mark, however, it is better than the activity showed against *Aspergillus niger* and *Penicillium digitatum*. It also demonstrated a zone of inhibition at 5.13 ± 1.10 mm against *Aspergillus fumigatus* and 4.24 ± 2.3 mm against *Trichophyton mentagrophytes*.

In case of yeasts, unprocessed silymarin recorded 8.0 ± 0.20 mm zone of inhibition against *Candida albicans* which is much higher than the 2.20 ± 0.32 mm diameter of the zone of inhibition it recorded against *Cryptococcus neoformans* showing a clear difference in sensitivity of the two pathogens when treated with unprocessed drug. The zone of inhibition was noted at 3.70 ± 0.48 mm against *Candida lusitaniae*. In the case of *Candida tropicalis*, the respective zone of inhibition was recorded at 4.02 ± 0.890 mm by the unprocessed silymarin which is nearly equal to the zone of inhibition (4.45 ± 0.17 mm) recorded against *Candida parapsilosis*. The zone of inhibition of unprocessed silymarin was noted as 3.73 ± 01.20 mm against *Candida krusei*.

Table 13. Antifungal activity of unprocessed silymarin, zone of inhibition (mm)

Antifungal activity of unprocessed silymarin					
Molds	Zone of inhibition	Amphotericin B	Yeasts	Zone of inhibition	Amphotericin B
<i>Aspergillus Niger</i>	3.01 ± 0.18	10.0 ± 0.20	<i>Candida albicans</i>	8.00 ± 0.20	25.0 ± 0.79
<i>Penicillium digitatum</i>	01.04 ± 0.1	11.0 ± 0.10	<i>Cryptococcus neoformans</i>	2.20 ± 0.32	13.0 ± 0.93
<i>Fusarium oxysporum</i>	4.70 ± 0.89	18.0 ± 1.01	<i>Candida lusitaniae</i>	3.70 ± 0.48	22.0 ± 0.05
<i>Trichophyton rubrum</i>	5.06 ± 0.10	32 ± 01.87	<i>Candida tropicalis</i>	4.02 ± 0.89	23.0 ± 1.21
<i>Aspergillus fumigates</i>	5.13 ± 1.10	31.1 ± 0.10	<i>Candida parapsilosis</i>	4.45 ± 0.17	23.0 ± 0.33
<i>Trichophyton mentagrophytes</i>	4.24 ± 2.3	17.80 ± 2.07	<i>Candida krusei</i>	3.73 ± 1.20	21.70 ± 1.40

The MIC and MFC values of unprocessed silymarin against different moulds and yeasts are shown in Tables 14 and 15 below. The MIC of unprocessed silymarin was recorded at 487 ± 0.130 mg/mL and its respective MFC at 511 ± 0.24 mg/mL against *Aspergillus niger*. It demonstrated 389 ± 0.32 mg/mL MIC and 482 ± 0.12 mg/mL MFC against *Penicillium digitatum*. The respective MIC and MFC values of unprocessed silymarin were recorded at 359 ± 0.22 mg/mL and 466 ± 0.41 mg/mL against *Fusarium oxysporum* and 372 ± 0.82 mg/mL and 437 ± 0.9 mg/mL respectively against *Trichophyton rubrum*. Similarly, the MIC and MFC values of unprocessed silymarin against *Aspergillus fumigatus* were recorded at 344 ± 3.1 mg/mL and 410 ± 0.86 mg/mL respectively. It also demonstrated the MIC value equal to 436 ± 3.89 mg/mL against *Trichophyton mentagrophytes* with the respective MFC value of 431 ± 0.73 mg/mL.

It required an MIC of 407.0 ± 4.1 mg/mL and MFC as 493.0 ± 6.2 mg/mL against *Candida albicans*, which are much higher than the MIC and MFC (436 ± 5.240 mg/mL and 498 ± 7.28 mg/mL respectively) values noted for *Cryptococcus neoformans* when tested with unprocessed silymarin. It shows a clear difference in the sensitivity levels of these pathogens when treated with unprocessed silymarin. Unprocessed silymarin MIC was noted at 398.0 ± 4.80 mg/mL against *Candida lusitaniae* with a respective MFC value of 439.0 ± 0.3 mg/mL and the MIC and MFC values were noted at 370.0 ± 04.9 mg/mL and 435.0 ± 0.9 mg/mL respectively against *Candida tropicalis*. The unprocessed silymarin MIC against *Candida parapsilosis* was recorded at 422 ± 3.43 mg/mL and its

respective MFC recorded at 502 ± 8.43 mg/mL against this pathogen. The MIC and MFC values against *Candida krusei* were recorded at 418 ± 0.43 mg/mL and 479 ± 0.08 mg/mL respectively. The MIC of unprocessed silymarin ranged from 344 ± 5.10 mg/mL to 487 ± 0.13 mg/mL. The lowest MIC of 344 ± 5.10 mg/mL was recorded against *Aspergillus fumigatus*, while the highest MIC (487 ± 0.13 mg/mL) was noted against *Aspergillus niger*. *Trichophyton mentagrophytes* required the second highest MIC value equal to 436 ± 3.43 mg/mL. All the organisms were found resistant to unprocessed silymarin out of which *Aspergillus niger* remained the most resistant one. The MFC values ranged from 410 ± 0.86 mg/mL to 511 ± 0.240 mg/mL. The lowest value of 410 ± 0.86 mg/mL was recorded against *Aspergillus fumigatus*, while the highest value of 511 ± 0.240 mg/mL was exhibited against *Aspergillus niger*. *Candida parapsilosis* had the second highest value (502 ± 4.43 mg/mL). All the organisms offered resistance to unprocessed silymarin and *Aspergillus niger* remained the most resistant fungus.

Table 14. Minimum Inhibitory Concentration of unprocessed silymarin (mg/mL)

Minimum Inhibitory Concentration of unprocessed silymarin (MIC)					
Molds	MIC	Amphotericin B	Yeasts	MIC	Amphotericin B
<i>Aspergillus Niger</i>	487 ± 0.13	25	<i>Candida albicans</i>	407.0 ± 9.1	100
<i>Penicillium digitatum</i>	389 ± 0.32	100	<i>Cryptococcus neoformans</i>	436 ± 5.24	12.54 ± 0.05
<i>Fusarium oxysporum</i>	359 ± 0.22	12.52 ± 0.34	<i>Candida lusitaniae</i>	398.0 ± 4.8	08 ± 0.92
<i>Trichophyton rubrum</i>	372 ± 0.82	5/11	<i>Candida tropicalis</i>	370.0 ± 4.9	7 ± 0.98
<i>Aspergillus fumigatus</i>	344 ± 5.100	2.40 ± 1.07	<i>Candida parapsilosis</i>	422 ± 6.43	15.0 ± 0.04
<i>Trichophyton mentagrophytes</i>	436 ± 3.89	0.350 ± 01.19	<i>Candida krusei</i>	418 ± 8.31	16 ± 0.22

Table 15. Minimum Fungicidal Concentration of unprocessed silymarin (mg/mL)

Minimum Fungicidal Concentration of unprocessed silymarin (MFC)					
Molds	MFC	Amphotericin B	Yeasts	MFC	Amphotericin B
<i>Aspergillus Niger</i>	511 ± 0.24	25 ± 0.9	<i>Candida albicans</i>	493.0 ± 6.2	30
<i>Penicillium digitatum</i>	482 ± 0.12	150	<i>Cryptococcus neoformans</i>	498 ± 7.28	50 ± 0.88
<i>Fusarium oxysporum</i>	466 ± 0.41	25 ± 0.92	<i>Candida lusitaniae</i>	439.0 ± 0.3	14.5 ± 0.18
<i>Trichophyton rubrum</i>	437 ± 0.90	11	<i>Candida tropicalis</i>	435.0 ± 0.9	28.0 ± 0.01
<i>Aspergillus fumigatus</i>	410 ± 0.86	7.4 ± 0.06	<i>Candida parapsilosis</i>	502 ± 8.43	16.0 ± 0.98
<i>Trichophyton mentagrophytes</i>	431 ± 0.73	0.650 ± 0.81	<i>Candida krusei</i>	479 ± 0.08	16.0 ± 0.09

SM-APSP showed enhanced antifungal activities than the unprocessed drug. It achieved 5.0 ± 0.16 mm and 2.10 ± 0.10 mm zones of inhibition against *Aspergillus niger* and *Penicillium digitatum* respectively. The diameter of the zone of inhibition against *Fusarium oxysporum* was noted at 8.2 ± 3.39 mm, and against *Trichophyton rubrum* at 9.30 ± 1.20 mm. *Aspergillus fumigatus* showed 9.44 ± 0.11 mm zone of inhibition and *Trichophyton mentagrophytes* showed 6.15 ± 1.30 mm zone of inhibition when treated with SM-APSP.

The diameter of the zone of inhibition of *Candida albicans* was noted at 12.48 ± 1.18 mm. Against *Cryptococcus neoformans*, SM-APSP recorded 3.70 ± 0.81 mm zone of inhibition and demonstrated 5.60 ± 0.83 mm of the zone of inhibition against *Candida lusitaniae*. The zone of inhibition against

Candida tropicalis was recorded at 5.70 ± 0.78 mm. Against *Candida parapsilosis* and *Candida krusei*, SM-APSP recorded 5.30 ± 1.130 mm and 5.20 ± 0.60 mm zones of inhibition respectively (Table 16).

Based on diameters of zone of inhibition, *Candida albicans* (12.48 ± 1.180 mm diameter of the zone of inhibition), *Aspergillus fumigatus* (9.44 ± 0.11 mm), and *Trichophyton rubrum* (9.3 ± 2.10 mm) were noted as the most sensitive fungi to SM-APSP. *Penicillium digitatum* proved as the most resistant pathogen in this experiment (Table 16).

Table 16. Antifungal activity of silymarin nanoparticles, zone of inhibition (mm)

Antifungal activity of silymarin nanoparticles					
Molds	Zone of inhibition (mm)	Amphotericin B	Yeasts	Zone of inhibition (mm)	Amphotericin B
Aspergillus Niger	5.0 ± 0.16	10.0 ± 0.07	<i>Candida albicans</i>	12.48 ± 1.18	25.0 ± 0.79
Penicillium digitatum	2.1 ± 0.1	11.0 ± 0.10	<i>Cryptococcus neoformans</i>	03.70 ± 0.81	13.0 ± 0.93
Fusarium oxysporum	8.20 ± 3.39	18.0 ± 1.01	<i>Candida lusitaniae</i>	05.6 ± 0.83	22.0 ± 0.05
Trichophyton rubrum	9.30 ± 1.20	32 ± 01.87	<i>Candida tropicalis</i>	05.7 ± 0.78	23.0 ± 1.21
Aspergillus fumigates	9.44 ± 0.11	31.1 ± 0.01	<i>Candida parapsilosis</i>	05.30 ± 1.13	23.0 ± 0.33
Trichophyton mentagrophytes	6.15 ± 1.30	11.02 ± 0.01	<i>Candida krusei</i>	5.20 ± 0.6	22.80 ± 0.14

The MIC and MFC results for SM-APSP are shown in Tables 17 and 18. The MICs of SM-APSP against *Aspergillus niger* and *Penicillium digitatum* were recorded at 342 ± 0.7 mg/mL and 354 ± 0.43 mg/mL respectively. For the same pathogens, the respective MFCs were noted at 464 ± 1.40 mg/mL and 388 ± 1.240 mg/mL. Similarly, the value of MIC and MFC were recorded at 334 ± 0.17 mg/mL and 360 ± 0.91 mg/mL against *Fusarium oxysporum* respectively. And 318 ± 0.610 mg/mL, 357 ± 1.790 mg/mL respectively against *Trichophyton rubrum*. Against *Aspergillus fumigatus*, SM-APSP recorded MIC and MFC values at 307 ± 0.83 mg/mL and 349 ± 3.74 mg/mL respectively. In the same way, it demonstrated MIC value of 320 ± 0.680 mg/mL against *Trichophyton mentagrophytes* with a respective MFC value of 351 ± 2.03 mg/mL.

SM-APSP recorded an MIC value of 366.1 ± 0.2 mg/mL and MFC value of 400 ± 4.7 mg/mL against *Candida albicans*. These values are lower than the MIC and MFC values (383 ± 0.36 mg/mL and 406 ± 4.12 mg/mL respectively) demonstrated by SM-APSP against *Cryptococcus neoformans*, showing the different sensitivity levels of these two pathogens when treated with SM-APSP. The MIC of SM-APSP against *Candida lusitaniae* was noted 333.2 ± 0.09 mg/mL, and its MFC as 364.9 ± 3.8 mg/mL. The MIC and MFC values against *Candida tropicalis* were recorded at 331.1 ± 0.9 mg/mL and 386 ± 5.30 mg/mL respectively. The MIC required by SM-APSP against *Candida parapsilosis* was noted at 387.2 ± 2.4 mg/mL, and its MFC was recorded at 404.4 ± 3.9 mg/mL against this pathogen. SM-APSP also recoded respective MIC and MFC values against *Candida krusei* at 360.1 ± 4.7 mg/mL and 394.4 ± 3.8 mg/mL.

The MIC values of SM-APSP ranged between 307 ± 0.83 and 387.2 ± 2.40 mg/mL, which are very low compared to the MIC values of unprocessed silymarin. The lowest MIC, 307 ± 0.83 mg/mL, was required against *Aspergillus fumigatus*. The highest of 387.20 ± 2.40 mg/mL was recorded against *Candida parapsilosis*. The MFC results (Table 18) for SM-APSP ranged between 349 ± 3.74 mg/mL and 464 ± 1.40 mg/mL. The MFC value of 349 ± 6.74 mg/mL, noted as the smallest was exhibited against *Aspergillus fumigatus*, while the highest MFC value of 464 ± 1.40 mg/mL was recorded against *Aspergillus niger*. The second highest MFC value of 406 ± 04.12 mg/mL was recorded against *Cryptococcus neoformans*. Upper MFC values compared to the corresponding

MIC value (Tables 17 and 18) are because a fungicidal agent may also act like a fungi static agent at lower concentrations.

Table 17. Minimum Inhibitory Concentration of silymarin nanoparticles (mg/mL)

Minimum Inhibitory Concentration of silymarin nanoparticles (MIC) mg/mL					
Molds	MIC	Amphotericin B	Yeasts	MIC	Amphotericin B
Aspergillus Niger	342 ± 0.70	24.0 ± 0.03	Candida albicans	366.1 ± 0.20	8
Penicillium digitatum	354 ± 0.43	100	Cryptococcus neoformans	383 ± 0.36	12.7 ± 0.05
Fusarium oxysporum	334 ± 0.17	12.3 ± 0.94	Candida lusitaniae	333.2 ± 0.09	08 ± 0.92
Trichophyton rubrum	318 ± 0.61	5	Candida tropicalis	331.1 ± 0.9	7 ± 0.98
Aspergillus fumigatus	307 ± 0.83	2.40 ± 1.07	Candida parapsilosis	387.2 ± 6.4	15.0 ± 0.04
Trichophyton mentagrophytes	320 ± 0.68	0.350 ± 01.19	Candida krusei	360.1 ± 4.7	16 ± 0.22

Table 18. Minimum Fungicidal Concentration of silymarin nanoparticles (mg/mL)

Minimum Fungicidal Concentration of silymarin nanoparticles (MFC) mg/mL					
Molds	MFC	Amphotericin B	Yeasts	MFC	Amphotericin B
Aspergillus Niger	464 ± 1.40	25 ± 0.9	Candida albicans	400 ± 5.70	30
Penicillium digitatum	388 ± 1.24	150	Cryptococcus neoformans	406 ± 6.12	50 ± 0.88
Fusarium oxysporum	360 ± 0.91	25 ± 0.92	Candida lusitaniae	364.9 ± 6.3	14.5 ± 0.18
Trichophyton rubrum	357 ± 1.79	11	Candida tropicalis	386 ± 5.30	28 ± 0.01
Aspergillus fumigatus	349 ± 6.74	7.4 ± 0.06	Candida parapsilosis	404.4 ± 7.3	16 ± 0.98
Trichophyton mentagrophytes	351 ± 7.03	0.650 ± 0.81	Candida krusei	394.4 ± 7.8	16.0 ± 0.09

In these experiments, the effects of unprocessed silymarin and SM-APSP against diverse microorganisms were determined and comparisons were drawn between the results obtained from the same concentrations of both the drugs. By comparing the zones of inhibition, MIC, MBC, and MFC of the samples with each other, it is clear that SM-APSP performed better than that of the unprocessed silymarin. It achieved higher diameters of zones of inhibition and required lower MIC, MBC, and MFC values against all tested pathogens. Our results also show that silymarin nanoparticles also demonstrated potent effects against some gram negative pathogens like *Enterobacter aerogenes* and *Klebsiella pneumonia*, with zones of inhibition diameters up to 12.0 ± 1.10mm and 09.4 ± 03.10mm respectively. It is important and very encouraging to note that the zones of inhibition, MIC, and MBC values against all these pathogens proved the enhanced antibacterial performance of SM-APSP. The data unequivocally shows that the antimicrobial activity of SM-APSP is much superior to that of unprocessed silymarin. All the tested microorganisms, including *A. niger*, *C. albicans*, and *Pseudomonas aeruginosa* showed an enhanced sensitivity to SM-APSP as compared to the unprocessed silymarin. The antimicrobial activity of silymarin nanoparticles surpassed the activity of unprocessed silymarin in each case. Converting silymarin to nanometer size enhanced its antimicrobial potential to an extent that we needed to use lower drug concentrations, with a reduction in MIC values by up to 50% in some cases.

The enhanced activity of SM-APSP and its improved performance was made possible after converting silymarin to nanometer size. Earlier research has also shown such results, in which nanoparticles prepared using other methods produced better results [92,93,94] (Mohammed,F.S.,2019) AND (Shah,S.M.M.,2011) AND (Latif,M.,2020).

Nanoparticles have increased penetration due to their extremely small diameters. They can better permeate the microbial cell membrane [83] (Gupta,R.,2020) via smaller holes, leading to their presence in higher concentrations and robust effects. Small sized particles with a larger surface-to-volume ratio can make available more proficient ways for antibacterial actions. Because nanoparticles have fine surfaces and nanometer sizes, they may use all of their surfaces in any direction to enter the bacterial cell membrane. The morphology of the particles can also affect their activity, and the SEM analysis has already proven the spherical shapes of our prepared nanoparticles. The infiltration of additional silymarin nanoparticles into microbial cells resulted in an increase in antibacterial activity and disruption of the bacterial cell membrane.

Converting a drug to the nanometer range can improve its solubility and absorption due to small size of the particles and a better wettability which increase its concentration at the required site leading to enhanced efficacy [44] (Sahibzada.,2017). The solubility experiments data also suggest the same because the nanoparticles showed improved and increased solubility. A better solubility and dissolution rate enhanced the effects of SM-APSP.

As the antimicrobial effectiveness is significantly increased, with the reduction in the particle size [95] (Yang,X.;2021), therefore, they can also stop those bacterial strains from growing, which otherwise, if left unchecked, may result in antibiotic resistance. The increased area of the surface to volume ratio of nanoparticles greatly contribute to their enhanced antimicrobial effects and when used as adjuncts, they can increase the activities of other antimicrobials, producing significantly enhanced results. The adjuvant antimicrobial therapy with such compounds may be very helpful [96] (Wang,D.,2018).

As currently used drugs possess various toxic effects, there is an exhaustive research program all over the globe to find novel natural antimicrobial drugs. Therefore, the encouraging findings from these experiments are important steps and can enable us to formulate these desperately needed drugs.

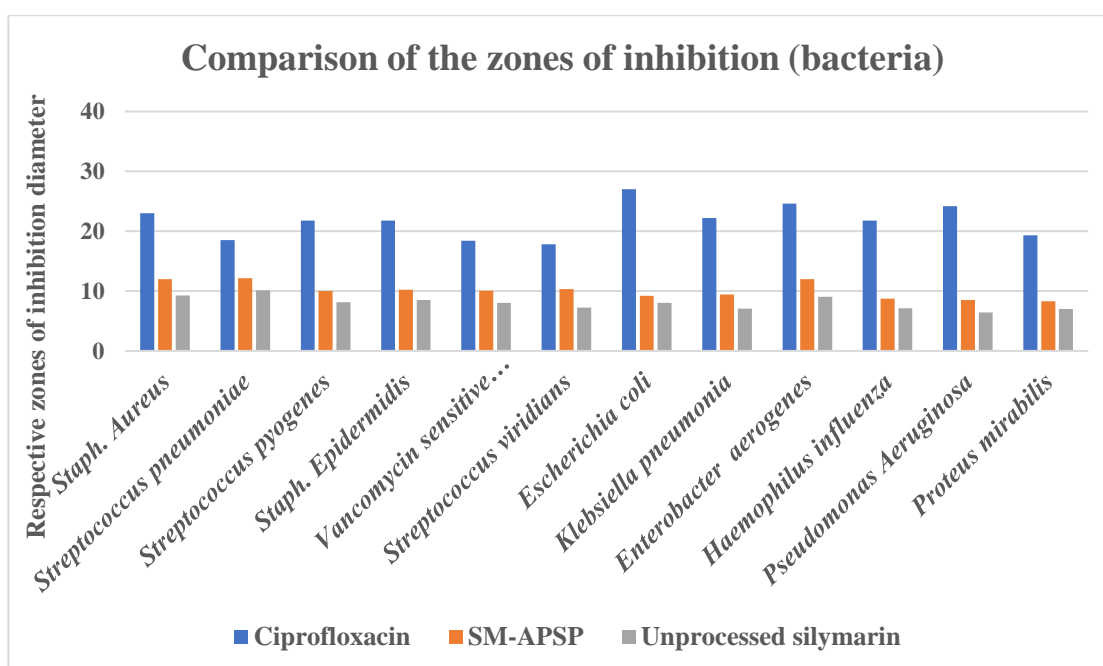


Figure 13. Comparison of zones of inhibition (bacteria) of SM-APSP, unprocessed silymarin, and ciprofloxacin

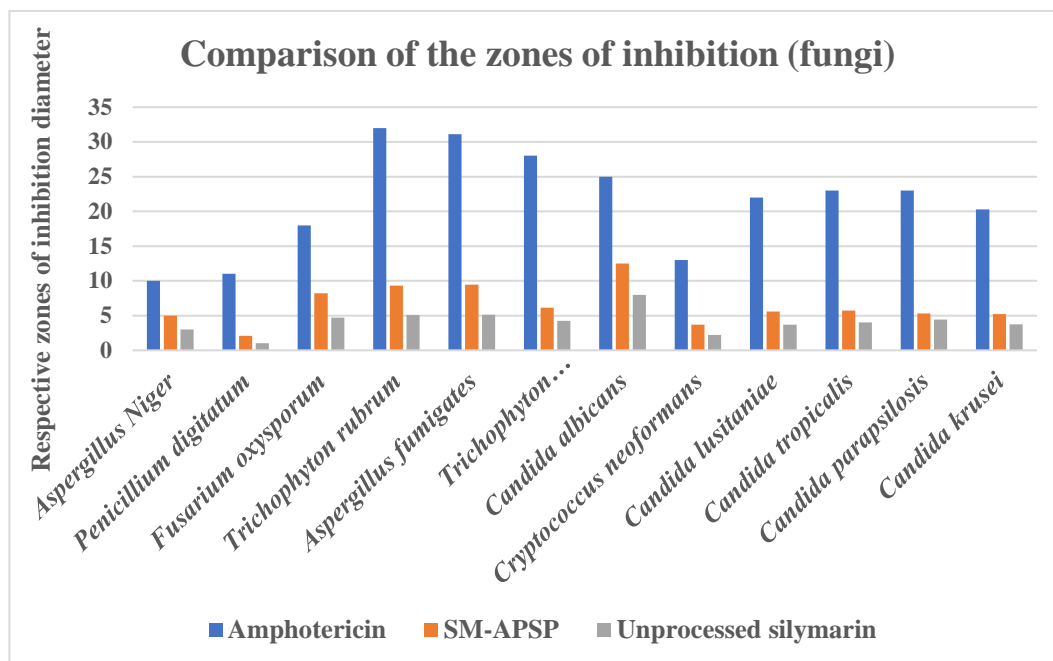


Figure 14. Comparison of the zones of inhibition (fungi) of SM-APSP, unprocessed silymarin, and amphotericin B

4. Conclusion

According to the present study, between APSP and EPN methods, APSP is the best method for the synthesis of silymarin nanoparticles. This is demonstrated by the characterization findings and, subsequently, by the silymarin nanoparticles' improved effects.

The solubility and dissolution of the prepared nanoparticles were many fold increase compared to their respective unprocessed drug. Due to their decreased particle size, the nano drug has been discovered to be more efficient against tested microorganisms than their unprocessed counterparts; therefore, the synergistic usage of naturally occurring compounds synthesized in the nanoparticle range in conjunction with antibiotics may provide positive outcomes. In comparison to silymarin that had not been processed, the nanoparticles' antioxidative properties were also significantly boosted.

It is recommended that clinical research be done on silymarin nanoparticles made using the APSP approach in light of the aforementioned information.

References

1. Khameneh B, Iranshahy M, Soheili V, Fazly Bazzaz BS. Review on plant antimicrobials: a mechanistic viewpoint. *Antimicrobial Resistance & Infection Control*, 8(1), 1-28 (2019).
2. Adamczak A, Ożarowski M, Karpiński TM. Antibacterial activity of some flavonoids and organic acids widely distributed in plants. *Journal of clinical medicine*, 9(1), 109-126 (2019).
3. Křen V, Valentová K. Silybin and its congeners: From traditional medicine to molecular effects. *Natural Product Reports*. 2022;39(6):1264-81.
4. Pendry BA, Kemp V, Hughes MJ, Freeman J, Nuhu HK, Sanchez-Medina A, Corcoran O, Galante E. Silymarin content in *Silybum marianum* extracts as a biomarker for the quality of commercial tinctures. *Journal of herbal medicine*, 10, 31-36 (2017).
5. Haghshenas B, Kiani A, Mansoori S, Mohammadi-Noori E, Nami Y. Probiotic properties and antimicrobial evaluation of silymarin-enriched *Lactobacillus* bacteria isolated from traditional curd. *Scientific Reports*. 2023 Jul 5;13(1):10916.
6. Abdelazim AS. Effect of silymarin as natural antioxidants and antimicrobial activity. *Egyptian Journal of Agricultural Research*. 2017 Jul 1;95(2):725-37.

7. Yun DG, Lee DG. Silymarin exerts antifungal effects via membrane-targeted mode of action by increasing permeability and inducing oxidative stress. *Biochimica et Biophysica Acta (BBA)-Biomembranes*, 1859(3), 467-74 (2017).
8. Alshehri FS, Kotb E, Nawaz M, Al-Jameel S, Amin KA. Preparation, characterization, and antibacterial competence of silymarin and its nano formulation. *Journal of Experimental Nanoscience*, 17(1), 100-12 (2022).
9. Askari F, Davoodi M, Ghelichli M, Asadi I, Jazideh F. The preventive effects of silymarin extract against *Streptococcus mutans* virulence and caries development in rat model and in vitro condition. *Eurasian Chemical Communications*, 2(12), 1164-71 (2020).
10. Ahmed A, Howladar S, Mohamed H, Al-Robai S. Phytochemistry, antimicrobial, anti-giardial and anti-amoebic activities of selected plants from Albaha area, Saudi Arabia. *British Journal of Medicine and Medical Research*, 18(11), 1-8 (2016).
11. Antika LD, Dewi RM. The pharmacological properties of silymarin and its constituents. *Natural Product Sciences*, 27(2), 68-77 (2021).
12. Adetuyi BO, Omolabi FK, Olajide PA, Oloke JK. Pharmacological, biochemical and therapeutic potential of milk thistle (silymarin): a review. *World News of Natural Sciences*, 37(2021), 75-91 (2021).
13. Surai PF. Silymarin as a natural antioxidant: an overview of the current evidence and perspectives. *Antioxidants*, 4(1), 204-47 (2015).
14. Akhtar DH, Iqbal U, Vazquez-Montesino LM, Dennis BB, Ahmed A. Pathogenesis of insulin resistance and atherogenic dyslipidemia in nonalcoholic fatty liver disease. *Journal of clinical and translational hepatology*, 7(4), 362-70 (2019).
15. Ismaili SA, Sayah K, Harhar H, Faouzi ME, Gharby S, Himmi B, Kitane S, El Belghiti MA. Chemical analysis and anti-oxidation activities of the Moroccan Milk Thistle. *Moroccan Journal of Chemistry*, 4(3), 4-3 (2016).
16. Choe U, Li Y, Gao B, Yu L, Wang TT, Sun J, Chen P, Yu LL. The chemical composition of a cold-pressed milk thistle seed flour extract, and its potential health beneficial properties. *Food & function*, 10(5), 2461-70 (2019).
17. Malekinejad H, Rezaabakhsh A, Rahmani F, Hobbenaghi R. Silymarin regulates the cytochrome P450 3A2 and glutathione peroxides in the liver of streptozotocin-induced diabetic rats. *Phytomedicine*, 19(7), 583-90 (2012).
18. Doğan D, Meydan İ, Kömüroğlu AU. Protective Effect of Silymarin and Gallic Acid against Cisplatin-Induced Nephrotoxicity and Hepatotoxicity. *International Journal of Clinical Practice*, 2022, 6541026- (2022).
19. Veisi S, Johari SA, Tyler CR, Mansouri B, Esmaeilbeigi M. Antioxidant properties of dietary supplements of free and nanoencapsulated silymarin and their ameliorative effects on silver nanoparticles induced oxidative stress in Nile tilapia (*Oreochromis niloticus*). *Environmental Science and Pollution Research*, 28(20), 26055-63 (2021).
20. Yardım A, Kucukler S, Özdemir S, Çomaklı S, Caglayan C, Kandemir FM, Çelik H. Silymarin alleviates docetaxel-induced central and peripheral neurotoxicity by reducing oxidative stress, inflammation and apoptosis in rats. *Gene*, 769, 145239 (2021).
21. Eskandari F, Momeni HR. Protective effect of silymarin on viability, motility and mitochondrial membrane potential of ram sperm treated with sodium arsenite. *International Journal of Reproductive BioMedicine*, 14(6), 397 (2016).
22. Abenavoli L, Izzo AA, Milić N, Cicala C, Santini A, Capasso R. Milk thistle (*Silybum marianum*): A concise overview on its chemistry, pharmacological, and nutraceutical uses in liver diseases. *Phytotherapy Research*, 32(11), 2202-13 (2018).
23. Zhu HJ, Brinda BJ, Chavin KD, Bernstein HJ, Patrick KS, Markowitz JS. An assessment of pharmacokinetics and antioxidant activity of free silymarin flavonolignans in healthy volunteers: a dose escalation study. *Drug Metabolism and Disposition*. 2013 Sep 1;41(9):1679-85.

24. Taran M, Safaei M, Karimi N, Almasi A. Benefits and application of nanotechnology in environmental science: an overview. *Biointerface Research in Applied Chemistry*, 11(1), 7860-70 (2021).
25. Vijayalakshmi K, Sivaraj D. Enhanced antibacterial activity of Cr doped ZnO nanorods synthesized using microwave processing. *RSC advances*. 2015;5(84):68461-9.
26. Pang Z, Raudonis R, Glick BR, Lin T-J, Cheng Z. Antibiotic resistance in *Pseudomonas aeruginosa*: mechanisms and alternative therapeutic strategies. *Biotechnology advances*. 2019;37(1):177-92.
27. Abuzar SM, Hyun SM, Kim JH, Park HJ, Kim MS, Park JS, Hwang SJ. Enhancing the solubility and bioavailability of poorly water-soluble drugs using supercritical antisolvent (SAS) process. *International journal of pharmaceutics*, 538(1-2), 1-3 (2018).
28. Alqahtani MS, Kazi M, Alsenaidy MA, Ahmad MZ. Advances in oral drug delivery. *Frontiers in pharmacology*, 12, 618411 (2021).
29. Parmar A, Sharma S. Engineering design and mechanistic mathematical models: standpoint on cutting edge drug delivery. *TrAC Trends in Analytical Chemistry*, 100, 15-35 (2018).
30. Sher M, Zahoor M, Shah SW, Khan FA. Is particle size reduction linked to drug efficacy: an overview into nano initiatives in pharmaceuticals. *Zeitschrift für Physikalische Chemie*. 2023 Jun 2(0).
31. Verma V, Ryan KM, Padrela L. Production and isolation of pharmaceutical drug nanoparticles. *International Journal of Pharmaceutics*, 603, 120708 (2021).
32. Recharla N, Riaz M, Ko S, Park S. Novel technologies to enhance solubility of food-derived bioactive compounds: A review. *Journal of Functional Foods*, 39, 63-73 (2017).
33. Sharma C, Desai MA, Patel SR. Effect of Process Parameters on Particle Size and Morphology of Telmisartan in Anti-solvent Crystallization. *Journal of the Institution of Engineers (India)*, 102(1), 163-74 (2021).
34. Jog R, Burgess DJ. Pharmaceutical amorphous nanoparticles. *Journal of pharmaceutical sciences*, 106(1), 39-65 (2017).
35. Khan FA, Zahoor M, Islam NU, Hameed R. Synthesis of Cefixime and Azithromycin Nanoparticles. *Journal of Nanomaterials*, 2016, 29-37 (2016).
36. Mohamed MS, Abdelhafez WA, Zayed G, Samy AM. Optimization, in-vitro release and in-vivo evaluation of gliquidone nanoparticles. *AAPS PharmSciTech*, 21(2), 1-2 (2020).
37. Kakran M, Sahoo NG, Tan IL, Li L. Preparation of nanoparticles of poorly water soluble antioxidant curcumin by antisolvent precipitation methods. *Journal of Nanoparticle Research*. 14(2012), 1-11 (2012).
38. Kakran M, Sahoo NG, Li L, Judeh Z. Fabrication of quercetin nanoparticles by anti-solvent precipitation method for enhanced dissolution. *Powder Technology*, 223(2012), 59-64 (2012).
39. Campodónico A, Collado E, Ricci R, Pappa H, Segall A, Pizzorno MT. Dissolution test for silymarin tablets and capsules. *Drug development and industrial pharmacy*, 27(3), 261-5 (2001).
40. Sharma S, Jaiswal S, Duffy B, Jaiswal AK. Nanostructured materials for food applications: spectroscopy, microscopy and physical properties. *Bioengineering*, 6(1), 26-42 (2019).
41. Racault C, Langlais F, Naslain R. Solid-state synthesis and characterization of the ternary phase Ti₃SiC₂. *Journal of materials Science*, 29(13), 3384-92 (2004).
42. Siekmann B, Westesen K. Thermoanalysis of the recrystallization process of melt-homogenized glyceride nanoparticles. *Colloids and surfaces B: Biointerfaces*, 3(3):159-75 (2004).
43. Khan BA, Rashid F, Khan MK, Alqahtani SS, Sultan MH, Almoshari Y. Fabrication of capsaicin loaded nanocrystals: Physical characterizations and in vivo evaluation. *Pharmaceutics*, 13(6), 841-854 (2021).
44. Sahibzada MU, Sadiq A, Khan S, Faidah HS, Naseemullah, Khurram M, Amin MU, Haseeb A. Fabrication, characterization and in vitro evaluation of silibinin nanoparticles: an attempt to enhance its oral bioavailability. *Drug Design, Development and Therapy*, 11(2017), 1453-64 (2017).

45. U.S. P. XXII "US Pharmacopeial convention" Rockville, Md 1788-1789 (1990).
46. Wu JW, Lin LC, Hung SC, Chi CW, Tsai TH. Analysis of silibinin in rat plasma and bile for hepatobiliary excretion and oral bioavailability application. *Journal of pharmaceutical and biomedical analysis*, 45(4), 635-41 (2007).
47. Yamaguchi T, Takamura H, Matoba T, Terao J. Method for the evaluation of the free radical-scavenging activity of foods by using 1, 1-diphenyl-2-picrylhydrazyl. *Bioscience, biotechnology, and biochemistry*, 62(6), 1201-4 (1998).
48. Doughari, J.H. Antimicrobial activity of *Tamarindus indica* Linn. *Trop. J. Pharm. Res.* 2006, 5(2), 597-603.
49. Di Costanzo A, Angelico R. Formulation strategies for enhancing the bioavailability of silymarin: the state of the art. *Molecules*, 24(11), 2155-83 (2019).
50. Németh Z, Csóka I, Semnani Jazani R, Sipos B, Haspel H, Kozma G, Kónya Z, Dobó DG. Quality by Design-Driven Zeta Potential Optimisation Study of Liposomes with Charge Imparting Membrane Additives. *Pharmaceutics*, 14(9), 1798-1822 (2022).
51. Mahapatra AP, Patil V, Patil R. Solubility enhancement of poorly soluble drugs by using novel techniques: A comprehensive review. *International Journal of PharmTech Research*, 13(2), 80-93 (2020).
52. Holder CF, Schaak RE. Tutorial on powder X-ray diffraction for characterizing nanoscale materials. *Acs Nano*, 13(7), 7359-65 (2019).
53. Tavano L, Alfano P, Muzzalupo R, de Cindio B. Niosomes vs microemulsions: new carriers for topical delivery of Capsaicin. *Colloids and surfaces B: Biointerfaces*, 87(2), 333-9 (2011).
54. Štukelj J, Svanbäck S, Agopov M, Löbmann K, Strachan CJ, Rades T, Yliruusi J. Direct measurement of amorphous solubility. *Analytical chemistry*, 91(11), 7411-7 (2019).
55. Bremmell KE, Prestidge CA. Enhancing oral bioavailability of poorly soluble drugs with mesoporous silica based systems: Opportunities and challenges. *Drug development and industrial pharmacy*, 45(3), 349-58 (2019).
56. Kakran M, Sahoo NG, Li L, Judeh Z, Wang Y, Chong K, Loh L. Fabrication of drug nanoparticles by evaporative precipitation of nanosuspension. *International journal of pharmaceutics*, 383(1-2), 285-92 (2010).
57. Albariqi AH, Chang RY, Tai W, Ke WR, Chow MY, Tang P, Kwok PC, Chan HK. Inhalable hydroxychloroquine powders for potential treatment of COVID-19. *Journal of Aerosol Medicine and Pulmonary Drug Delivery*, 34(1), 20-31 (2021).
58. Yingchoncharoen P, Kalinowski DS, Richardson DR. Lipid-based drug delivery systems in cancer therapy: what is available and what is yet to come. *Pharmacological reviews*, 68(3), 701-87 (2016).
59. Yousaf AM, Malik UR, Shahzad Y, Mahmood T, Hussain T. Silymarin-laden PVP-PEG polymeric composite for enhanced aqueous solubility and dissolution rate: preparation and in vitro characterization. *Journal of pharmaceutical analysis*, 9(1), 34-9 (2019).
60. Croissant JG, Butler KS, Zink JJ, Brinker CJ. Synthetic amorphous silica nanoparticles: toxicity, biomedical and environmental implications. *Nature Reviews Materials*, 5(12), 886-909 (2020).
61. Ali I, Ullah S, Imran M, Saifullah S, Hussain K, Kanwal T, Nisar J, Shah MR. Synthesis of biocompatible triazole based non-ionic surfactant and its vesicular drug delivery investigation. *Chemistry and Physics of Lipids*, 228(2020), 104894-104894 (2020).
62. Shah SM, Ullah F, Khan S, Shah SM, de Matas M, Hussain Z, Minhas MU, AbdEl-Salam NM, Assi KH, Isreb M. Smart nanocrystals of artemether: fabrication, characterization, and comparative in vitro and in vivo antimalarial evaluation. *Drug design, development and therapy*, 10(2016), 3837-50 (2016).
63. Kayaert P, Van den Mooter G. Is the amorphous fraction of a dried nanosuspension caused by milling or by drying? A case study with Naproxen and Cinnarizine. *European journal of pharmaceutics and biopharmaceutics*, 81(3), 650-6 (2012).

64. Da Silva FL, Marques MB, Kato KC, Carneiro G. Nanonization techniques to overcome poor water-solubility with drugs. *Expert opinion on drug discovery*, 15(7), 853-64 (2020).
65. Chi Lip Kwok P, Chan HK. Nanotechnology versus other techniques in improving drug dissolution. *Current pharmaceutical design*, 20(3), 474-82 (2014).
66. Kumar M, Shanthi N, Mahato AK, Soni S, Rajnikanth PS. Preparation of luliconazole nanocrystals loaded hydrogel for improvement of dissolution and antifungal activity. *Heliyon*, 5(5), e01688-e01688 (2019).
67. Pestovsky YS, Martínez-Antonio A. "Gold Nanoparticles with Immobilized β -cyclodextrin-capsaicin Inclusion Complex for Prolonged Capsaicin Release." *IOP Conference Series: Materials Science and Engineering*, (Vol. 389, No. 1, p. 012030) (2018).
68. Upadhyay P, Bhattacharjee M, Bhattacharya S, Ahir M, Adhikary A, Patra P. Silymarin-loaded, lactobionic acid-conjugated porous PLGA nanoparticles induce apoptosis in liver cancer cells. *ACS Applied Bio Materials*, 3(10), 7178-92 (2020).
69. Piwowarczyk L, Kucinska M, Tomczak S, Mlynarczyk DT, Piskorz J, Goslinski T, Murias M, Jelinska A. Liposomal Nanoformulation as a Carrier for Curcumin and pEGCG—Study on Stability and Anticancer Potential. *Nanomaterials*, 12(8), 1274 (2022).
70. Pande VV, Abhale VN, Möschwitzer JP. Nanocrystal technology: a particle engineering formulation strategy for the poorly water soluble drugs. *International Journal of Pharmaceutics*, 453(1), 126-41 (2016).
71. Voorhees PW. The theory of Ostwald ripening. *Journal of Statistical Physics*, 38(1/2), 231-52 (1985).
72. Kumar D, Lashari N, Ganat T, Ayoub MA, Soomro AA, Chandio TA. A review on application of nanoparticles in cEOR: Performance, mechanisms, and influencing parameters. *Journal of Molecular Liquids*, 353(2022), 118821 (2022).
73. Kaushik M, Niranjana R, Thangam R, Madhan B, Pandiyarasan V, Ramachandran C, Oh DH, Venkatasubbu GD. Investigations on the antimicrobial activity and wound healing potential of ZnO nanoparticles. *Applied Surface Science*, 479(2019), 1169-77 (2019).
74. Kesisoglou F, Panmai S, Wu Y. Nanosizing—oral formulation development and biopharmaceutical evaluation. *Advanced drug delivery reviews*. 2007 Jul 30;59(7):631-44.
75. Bhujbal SV, Mitra B, Jain U, Gong Y, Agrawal A, Karki S, Taylor LS, Kumar S, Zhou QT. Pharmaceutical amorphous solid dispersion: A review of manufacturing strategies. *Acta Pharmaceutica Sinica B*, 11(8), 2505-36 (2021).
76. Tvrdý V, Pourová J, Jirkovský E, Křen V, Valentová K, Mladěnka P. Systematic review of pharmacokinetics and potential pharmacokinetic interactions of flavonolignans from silymarin. *Medicinal Research Reviews*, 41(4), 2195-246 (2021).
77. Abdullah AS, Sayed IE, El-Torgoman AM, Kalam A, Wageh S, Kamel MA. Green Synthesis of silymarin–chitosan nanoparticles as a new nano formulation with enhanced anti-fibrotic effects against liver fibrosis. *International Journal of Molecular Sciences*, 23(10), 5420-5420 (2022).
78. Javed S, Kohli K, Ali M. Reassessing bioavailability of silymarin. *Alternative medicine review*, 16(3), 239-49 (2011).
79. Pradhan R, Lee DW, Choi HG, Yong CS, Kim JO. Fabrication of a uniformly sized fenofibrate microemulsion by membrane emulsification. *Journal of microencapsulation*, 30(1), 42-8 (2013).
80. Sahibzada MU, Sadiq A, Zahoor M, Naz S, Shahid M, Qureshi NA. Enhancement of bioavailability and hepatoprotection by silibinin through conversion to nanoparticles prepared by liquid antisolvent method. *Arabian Journal of Chemistry*, 13(2), 3682-9 (2020).
81. Hedaya M, Bandarkar F, Nada A. In vitro and in vivo evaluation of ibuprofen nanosuspensions for enhanced oral bioavailability. *Medical Principles and Practice*, 30(4), 361-8 (2021).
82. Sahibzada MU, Zahoor M, Sadiq A, ur Rehman F, Al-Mohaimed AM, Shahid M, Naz S, Ullah R. Bioavailability and hepatoprotection enhancement of berberine and its nanoparticles prepared by liquid antisolvent method. *Saudi Journal of Biological Sciences*, 28(1), 327-32 (2021).

83. Gupta R, Badhe Y, Mitragotri S, Rai B. Permeation of nanoparticles across the intestinal lipid membrane: dependence on shape and surface chemistry studied through molecular simulations. *Nanoscale*, 12(11), 6318-33 (2020).
84. Muflihah YM, Gollavelli G, Ling YC. Correlation study of antioxidant activity with phenolic and flavonoid compounds in 12 Indonesian indigenous herbs. *Antioxidants*, 10(10), 1530-1544 (2021).
85. Sora GT, Haminiuk CW, da Silva MV, Zielinski AA, Gonçalves GA, Bracht A, Peralta RM. A comparative study of the capsaicinoid and phenolic contents and in vitro antioxidant activities of the peppers of the genus *Capsicum*: An application of chemometrics. *Journal of food science and technology*, 52(12), 8086-94 (2015).
86. Li F, Boateng ID, Yang XM, Li Y, Liu W. Effects of processing methods on quality, antioxidant capacity, and cytotoxicity of *Ginkgo biloba* leaf tea product. *Journal of the Science of Food and Agriculture*, 103(10), 4993-5003 (2023).
87. Khanpara P, Vaishnav I. A complete review on traditional Healers-Punarnava. *Journal of Medicinal Plants Studies*, 10(5), 141-149 (2022).
88. Asgharpour M, Alirezaei A. Herbal antioxidants in dialysis patients: a review of potential mechanisms and medical implications. *Renal failure*, 43(1), 351-61 (2021).
89. Hegazy AM, El-Sayed EM, Ibrahim KS, Abdel-Azeem AS. Dietary antioxidant for disease prevention corroborated by the Nrf2 pathway. *Journal of Complementary and Integrative Medicine*, 16(3), [2018-0161](#) (2019).
90. Zimmer AR, Leonardi B, Miron D, Schapoval E, de Oliveira JR, Gosmann G. Antioxidant and anti-inflammatory properties of *Capsicum baccatum*: from traditional use to scientific approach. *Journal of Ethnopharmacology*, 139(1), 228-33 (2012).
91. Arampatzis DA, Karkanis AC, Tsiropoulos NG. Silymarin content and antioxidant activity of seeds of wild *Silybum marianum* populations growing in Greece. *Annals of Applied Biology*, 174(1), 61-73 (2019).
92. Mohammed FS, Pehlivan M, Sevindik M. Antioxidant, antibacterial and antifungal activities of different extracts of *Silybum marianum* collected from Duhok (Iraq). *International Journal of Secondary Metabolites*, 6(4), 317-22 (2019).
93. Shah SM, Khan FA, Shah SM, Chishti KA, Pirzada SM, Khan MA, Farid A. Evaluation of phytochemicals and antimicrobial activity of white and blue capitulum and whole plant of *Silybum marianum*. *World Applied Sciences Journal*, 12(8), 1139-44 (2011).
94. Latif M, Umar M, Ihtisham, Rahim A, Khan S, Ali, Fatima N, Hussain I, et al.. Isolation and biological evaluation of some secondary metabolites from seeds of *Silybum marianum*. *Pharmacognosy Magazine*, 16(68), 93-98 (2020).
95. Yang, X.; Chung, E.; Johnston, I.; Ren, G.; Cheong, Y.-K. Exploitation of Antimicrobial Nanoparticles and Their Applications in Biomedical Engineering. *Appl. Sci.* **2021**, *11*, 4520.
96. Wang D, Xie K, Zou D, Meng M, Xie M. Inhibitory effects of silybin on the efflux pump of methicillin-resistant *Staphylococcus aureus*. *Molecular medicine reports*, 18(1), 827-33 (2018).